Inorg. Chem. **2008**, *47*, 9624−9641

Synthesis, Structure, and Reactivity of Ruthenium Carboxylato and 2-Oxocarboxylato Complexes Bearing the Bis(3,5-dimethylpyrazol-1-yl)acetato Ligand

Stefan Tampier,[†,‡] Rainer Müller,[‡,§] Andrea Thorn,[†] Eike Hübner,[†] and Nicolai Burzlaff*[,†]

Inorganic Chemistry, Department of Chemistry and Pharmacy & Interdisciplinary Center for Molecular Materials (ICMM), University of Erlangen-Nürnberg, Egerlandstraße 1, D-91058 Erlangen, Germany, and Department of Chemistry, University of Konstanz, Fach M728, D-78457 Konstanz, Germany

Received January 4, 2008

A series of ruthenium(II) acetonitrile, pyridine (py), carbonyl, SO_2, and nitrosyl complexes [Ru(bdmpza)(O_2CR)(L)(PPh_3)] (L = NCMe, py, CO, SO_2) and [Ru(bdmpza)(O_2CR)(L)(PPh_3)]BF_4 (L = NO) containing the bis(3,5-dimethylpyrazol-1-yl)acetato (bdmpza) ligand, a *N,N,O* heteroscorpionate ligand, have been prepared. Starting from ruthenium chlorido, carboxylato, or 2-oxocarboxylato complexes, a variety of acetonitrile complexes [Ru(bdmpza)Cl(NCMe)(PPh_3)] (**4**) and [Ru(bdmpza)(O_2CR)(NCMe)(PPh_3)] (R = Me (**5a**), R = Ph (**5b**)), as well as the pyridine complexes [Ru(bdmpza)Cl(PPh_3)(py)] (**6**) and [Ru(bdmpza)(O_2CR)(PPh_3)(py)] (R = Me (**7a**), R = Ph (**7b**), R = (CO)Me (**8a**), R = (CO)Et (**8b**), R = (CO)Ph) (**8c**)), have been synthesized. Treatment of various carboxylato complexes [Ru(bdmpza)(O_2CR)(PPh_3)$_2$] (R = Me (**2a**), Ph (**2b**)) with CO afforded carbonyl complexes [Ru(bdmpza)(O_2CR)(CO)(PPh_3)] (**9a**, **9b**). In the same way, the corresponding sulfur dioxide complexes [Ru(bdmpza)(O_2CMe)(PPh_3)(SO_2)] (**10a**) and [Ru(bdmpza)(O_2CPh)(PPh_3)(SO_2)] (**10b**) were formed in a reaction of the carboxylato complexes with gaseous SO_2. None of the 2-oxocarboxylato complexes [Ru(bdmpza)(O_2C(CO)R)(PPh_3)$_2$] (R = Me (**3a**), Et (**3b**), Ph (**3c**)) showed any reactivity toward CO or SO_2, whereas the nitrosyl complex cations [Ru(bdmpza)(O_2CMe)(NO)(PPh_3)]$^+$ (**11**) and [Ru(bdmpza)(O_2C(CO)Ph)(NO)(PPh_3)]$^+$ (**12**) were formed in a reaction of the acetato **2a** or the benzoylformato complex **3c** with an excess of nitric oxide. Similar cationic carboxylato nitrosyl complexes [Ru(bdmpza)(O_2CR)(NO)(PPh_3)]BF_4 (R = Me (**13a**), R = Ph (**13b**)) and 2-oxocarboxylato nitrosyl complexes [Ru(bdmpza)(O_2C(CO)R)(NO)(PPh_3)]BF_4 (R = Me (**14a**), R = Et (**14b**), R = Ph (**14c**)) are also accessible via a reaction with NO[BF_4]. X-ray crystal structures of the chlorido acetonitrile complex [Ru(bdmpza)Cl(NCMe)(PPh_3)] (**4**), the pyridine complexes [Ru(bdmpza)(O_2CMe)(PPh_3)(py)] (**7a**) and [Ru(bdmpza)(O_2CC(O)Et)(PPh_3)(py)] (**8b**), the carbonyl complex [Ru(bdmpza)(O_2CPh)(CO)(PPh_3)] (**9b**), the sulfur dioxide complex [Ru(bdmpza)(O_2CPh)(PPh_3)(SO_2)] (**10b**), as well as the nitrosyl complex [Ru(bdmpza)(O_2C(CO)Me)(NO)(PPh_3)]BF_4 (**14a**), are reported. The molecular structure of the sulfur dioxide complex [Ru(bdmpza)(O_2CPh)(PPh_3)(SO_2)] (**10b**) revealed a rather unusual intramolecular SO_2−O_2CPh Lewis acid−base adduct.

Introduction

Bis(pyrazol-1-yl)acetic acids, such as bis(3,5-dimethylpyrazol-1-yl)acetic acid (Hbdmpza) introduced 1999 by A. Otero,[1] are available in a broad spectrum of chiral and achiral ligands and thus have been subject of two very recent reviews by Otero and Pettinari.[1,2] Complexes of these *N,N,O* donor ligands with various transition metal complexes reveal their potential in organometallic and coordination chemistry as scorpionate ligands closely related to Tp.[1,2] Lately, we reported on ruthenium(II) complexes bearing the bdmpza

* To whom correspondence should be addressed. E-mail: burzlaff@chemie.uni-erlangen.de. Phone: +49(0)9131/85-28976. Fax: +49(0)9131/85-27387.
† University of Erlangen-Nürnberg.
‡ Both authors contributed equally to this work.
§ University of Konstanz.

(1) Otero, A.; Fernańdez-Baeza, J.; Antinõlo, A.; Tejeda, J.; Lara-Sańchez, A. *Dalton Trans.* **2004**, 1499–1510.
(2) Pettinari, C.; Pettinari, R. *Coord. Chem. Rev.* **2005**, *249*, 663–691.

10.1021/ic8000224 CCC: $40.75
Published on Web 09/19/2008

ligand such as [Ru(bdmpza)Cl(PPh_3)$_2$] (**1**).[3] Because of the sterical hindrance of the bdmpza ligand, one of the PPh_3 ligands and the chlorido ligand can easily be exchanged for carboxylato or cumulynidene ligands.[3,4] Other ruthenium complexes bearing the bdmpza ligand have recently been reported by Cao and Otero.[5] The carboxylato complexes [Ru(bdmpza)(O_2CR)(PPh_3)] (**2a**: R = Me; **2b**: R = Ph) and the 2-oxocarboxylato complexes [Ru(bdmpza)($O_2C(CO)R$)-(PPh_3)] (**3a**: R = Me; **3b**: R = Et; **3c**: R = Ph) showed significant tendencies for a hemilabile κ^1O^1-behavior regarding the $\kappa^2O^1,O^{1'}$-carboxylato and κ^2O^1,O^2-2-oxocarboxylato ligands.[3] As a proof for these hemilabile ligands, we recently reported on a water adduct [Ru(bdmpza)(O_2CMe)(OH_2)-(PPh_3)] (**2a** × H_2O) and an acetonitrile complex [Ru-(bdmpza)($O_2C(CO)Ph$)(NCMe)(PPh_3)] (**3c** × NCMe).[3b] Ruthenium(II) complexes with hemilabile ligands, as well as with coordinated solvent molecules, are often key compounds in inorganic syntheses or catalytic reactions. A recent example is the ruthenium hydridotris(pyrazolyl)borate (Tp) complex [RuTpH(NCMe)(PPh_3)], which exhibits catalytic activity for the hydrogenation of CO_2 to formic acid and is easily derived from [RuTpCl(NCMe)(PPh_3)].[6] Thus, inspired by [RuTpCl(PPh_3)(MeCN)] we decided to study the coordination of acetonitrile and pyridine by various ruthenium(II) complexes bearing the bdmpza ligand. Furthermore, 16 VE complex fragments coordinating small molecules often allow the syntheses and stabilization of otherwise highly reactive molecules in the complex environment. As an example the synthesis of sulfene complexes starting from ruthenium SO_2 complexes should be mentioned.[7] Therefore, here we study also the coordination of small molecules CO, NO, and especially SO_2 that might act as π acceptor ligands L in ruthenium complexes [Ru(bdmpza)(O_2CR)(L)(PPh_3)] (L = CO, SO_2, NO).

Experimental Section

All experiments were carried out with Schlenk technique under an argon atmosphere. Solvents were dried by distillation over suitable drying agents [THF (Na), Et_2O (Na), pentane ($LiAlH_4$), hexane (Na), CH_2Cl_2 (CaH_2)] prior to use and were stored under Argon. IR: Biorad FTS 60, CaF_2 cuvets (0.5 mm) or KBr matrix. ^{1}H NMR and ^{13}C NMR: Bruker AC 250, Bruker DRX 600 Avance and Varian Unity Inova 400. ^{31}P NMR: JEOL GX 400 and Varian Unity Inova 400. 2D NMR experiments: Bruker DRX 600 Avance. δ values are given relative to TMS (^{1}H), solvent peaks (^{13}C) or to triphenylphosphine at −4.72 ppm as internal standard (^{31}P). FAB MS: modified Finnigan MAT 312. Elemental analyses: Analytical Laboratory of the Department of Chemistry, University of Konstanz or Euro EA 3000 (Euro Vector) and EA 1108 (Carlo Erba) ($\sigma \pm$ 1% of the measured content). A modified Siemens P4 and an Enraf-Nonius CAD 4 Mach 3 diffractometer were used for X-ray structure determination. The syntheses of [Ru(bdmpza)Cl(PPh_3)$_2$] (**1**), the ruthenium carboxylato complexes [Ru(bdmpza)(O_2CR)(PPh_3)] (**2a**: R = Me, **2b**: R = Ph) and the ruthenium 2-oxocarboxylato complexes [Ru(bdmpza)($O_2CC(O)R$)(PPh_3)] (**3a**: R = Me, **3b**: R = Ph, **3c**: R = Et, **3d**: R = $CH_2CH_2CO_2H$) were reported recently.[3] To remove last traces of thallous carboxylate the acetato and benzoato complexes **2a** and **2b** were recrystallized from CH_2Cl_2/pentane. All the 2-oxocarboxylato complexes used for experiments had been synthesized by using this crystalline complex **2a**. Acetonitrile and pyridine have been distilled prior to use. Nitrogen oxide, carbon monoxide, carbon dioxide, nitrogen and sulfur dioxide were used as purchased. For differentiation of the NMR data the signals of the bdmpza ligand next to the PPh_3 ligand are marked without an apostrophe.

Method A: General Procedure for the Syntheses of Acetonitrile Complexes. The chlorido, acetato, or benzoato complexes **1**, **2a**, or **2b** were dissolved in acetonitrile, and the reaction mixture was stirred at ambient temperature. The progress of the reaction was monitored by IR spectroscopy. After the reaction was completed, the solvent was reduced in vacuo until precipitation occurred. Precipitation was completed by adding pentane. The product was filtered off and dried in vacuo.

[Ru(bdmpza)Cl(NCMe)(PPh_3)] (4). Reaction of [Ru(bdmpza)Cl(PPh_3)$_2$] (**1**) (0.428 g, 0.471 mmol) with acetonitrile (20 mL) for 4 h according to method A but with heating under reflux afforded [Ru(bdmpza)Cl(NCMe)(PPh_3)] (**4**) as a yellow crystalline powder.

Yield 0.301 g (0.438 mmol, 93%). mp 230 °C (dec.). IR (CH_2Cl_2): $\tilde{\nu}$ = 2275 w (C≡N), 2254 vw, 1660 vs (CO_2^-), 1647 sh, 1565 w (C=N), 1483 w, 1463 vw, 1434 m, 1420 w cm^{-1}. IR (KBr): $\tilde{\nu}$ = 2269 w (C≡N), 2247 vw, 1657 vs (CO_2^-), 1642 sh, 1583 vw, 1561 m (C=N), 1483 w, 1460 vw, 1433 m, 1416 vw cm^{-1}. UV/vis (CH_2Cl_2): λ_{max}/nm (log ε) = 237.0 (4.34), 267.0 (3.91), 274.0 (3.90). FAB-MS (NBOH-matrix): *m*/*z* (%) = 686 (10) [M^+], 645 (100) [M^+ − MeCN], 610 (33) [M^+ − MeCN − Cl], 566 (29) [M^+ − MeCN − Cl − CO_2], 363 (38) [M^+ − MeCN − Cl − bdmpza]. ^{1}H NMR ($CDCl_3$, 400 MHz): δ = 1.88 (s, 3H, NC-CH_3), 1.88 (s, 3H, $C^{3'}$-CH_3), 2.47 (s, 3H, C^5−CH_3), 2.51 (s, 3H, $C^{5'}$-CH_3), 2.71 (s, 3H, C^3−CH_3), 5.89 (s, 1H, H_{pz}), 6.04 (s, 1H, $H_{pz'}$), 6.51 (s, 1H, CH), 7.26 (m, 6H, *m*-PPh_3), 7.28 (m, 3H, *p*-PPh_3), 7.30 (m, 6H, *o*-PPh_3) ppm. ^{13}C NMR ($CDCl_3$, 100.5 MHz): δ = 3.67 (NC-CH_3), 10.9 ($C^{5'}$-CH_3), 11.4 (C^5−CH_3), 14.4 ($C^{3'}$-CH_3), 15.0 (C^3−CH_3), 69.1 (CH), 108.6 (d, $C^{4'}$, $^4J_{CP}$ = 2.8 Hz), 108.8 (C^4), 124.0 (CN), 127.4 (d, *m*-PPh_3, $^3J_{CP}$ = 9.2 Hz), 129.0 (d, *p*-PPh_3, $^3J_{CP}$ = 1.8 Hz), 134.3 (d, *o*-PPh_3, $^2J_{CP}$ = 9.5 Hz), 134.7 (d, *i*-PPh_3, $^1J_{CP}$ = 40.7 Hz), 140.3 (d, $C^{5'}$, $^5J_{CP}$ = 1.0 Hz), 141.6 (C^5), 155.2 (d, $C^{3'}$, $^3J_{CP}$ = 2.6 Hz), 158.4 (C^3), 167.6 (CO_2^-) ppm. ^{31}P NMR ($CDCl_3$, 161.8 MHz): δ = 48.8 ppm. Anal. Calcd for $C_{32}H_{33}ClN_5O_2PRu$ (687.14): C, 55.93; H, 4.84; N, 10.19. Found C, 55.87; H, 4.76; N, 10.06.

[Ru(bdmpza)(O_2CMe)(NCMe)(PPh_3)] (5a). Reaction of [Ru(bdmpza)(O_2CMe)(PPh_3)] (**2a**) (0.134 g, 0.200 mmol) with acetonitrile (10 mL) for 5 h according to method A afforded

(3) (a) López-Hernández, A.; Müller, R.; Kopf, H.; Burzlaff, N. *Eur. J. Inorg. Chem.* **2002**, 671–677. (b) Müller, R.; Hübner, E.; Burzlaff, N. *Eur. J. Inorg. Chem.* **2004**, 2151–2159.
(4) Kopf, H.; Pietraszuk, C.; Hübner, E.; Burzlaff, N. *Organometallics* **2006**, *25*, 2533–2546.
(5) (a) Ortiz, M.; Díaz, A.; Cao, R.; Otero, A.; Fernández-Baeza, J. *Inorg. Chim. Acta* **2004**, *357*, 19–24. (b) Ortiz, M.; Díaz, A.; Cao, R.; Suardíaz, R.; Otero, A.; Antinõlo, A.; Fernández-Baeza, J. *Eur. J. Inorg. Chem.* **2004**, 3353–3357.
(6) (a) Chan, W.-C.; Lau, C. P.; Chen, Y.-Z.; Fang, Y.-Q.; Ng, S. M.; Jia, G. *Organometallics* **1997**, *16*, 34–44. (b) Yin, C.; Xu, Z.; Yang, S.-Y.; Ng, S. M.; Wong, K. Y.; Lin, Z.; Lau, C. P. *Organometallics* **2001**, *20*, 1216–1222. (c) Ng, S. M.; Yin, C.; Yeung, C. H.; Chan, T. C.; Lau, C. P. *Eur. J. Inorg. Chem.* **2004**, 1788–1793. (d) Lau, C. P.; Ng, S. M.; Jia, G.; Lin, Z. *Coord. Chem. Rev.* **2007**, *251*, 2223–2237.
(7) (a) Schenk, W. A.; Urban, P.; Dombrowski, E. *Chem. Ber.* **1993**, *126*, 679–684. (b) Schenk, W. A.; Bezler, J.; Burzlaff, N.; Hagel, M.; Steinmetz, B. *Eur. J. Inorg. Chem.* **2000**, 287–297.

[Ru(bdmpza)(O_2CMe)(NCMe)(PPh_3)] (**5a**) as a yellow crystalline powder.

Yield 0.141 g (0.198 mmol, 99%). mp 145 °C (dec). IR (CH_2Cl_2): $\tilde{\nu}$ = 2271 w (C≡N), 1663 vs (CO_2^-), 1648 sh, 1608 m, 1591 sh, 1564 w (C=N), 1484 w, 1464 vw, 1434 m, 1417 vw cm^{-1}. IR (KBr): $\tilde{\nu}$ = 2263 m (C≡N), 1659 vs (CO_2^-), 1606 s, 1587 sh, 1564 w (C=N), 1483 w, 1463 vw, 1434 m, 1417 vw cm^{-1}. UV/vis (CH_2Cl_2): λ_{max}/nm (log ε) = 236.0 (4.36), 268.0 (3.91), 275.0 (3.90), 289.0 (3.88). FAB-MS (NBOH-matrix): *m*/*z* (%) = 711 (8) [M^+], 651 (97) [$M^+ - HO_2CMe$], 610 (100) [$M^+ - HO_2CMe$ − MeCN], 565 (46) [$M^+ - HO_2CMe - CO_2$ − MeCN − H]. ^{1}H NMR ($CDCl_3$, 400 MHz): δ = 1.31 (s, 3H, OAc-CH_3), 1.56 (s, 3H, C^3−CH_3), 2.22 (s, 3H, NC-CH_3), 2.43 (s, 3H, $C^{3'}$-CH_3), 2.47 (s, 3H, $C^{5'}$-CH_3), 2.54 (s, 3H, C^5−CH_3), 5.91 (s, 1H, H_{pz}), 6.07 (s, 1H, $H_{pz'}$), 6.55 (s, 1H, CH), 7.10−7.50 (m, 15H, PPh_3) ppm. ^{13}C NMR ($CDCl_3$, 62.9 MHz): δ = 4.60 (NC-CH_3), 11.0 ($C^{5'}$-CH_3), 11.6 (C^5−CH_3), 13.3 ($C^{3'}$-CH_3), 14.2 (C^3−CH_3), 23.8 (OAc-CH_3), 69.7 (CH), 108.2 (d, $C^{4'}$, $^4J_{CP}$ = 2.9 Hz), 108.4 (C^4), 124.7 (CN), 127.5 (d, *m*-PPh_3, $^3J_{CP}$ = 9.3 Hz), 128.9 (*p*-PPh_3), 134.7 (d, *o*-PPh_3, $^2J_{CP}$ = 9.7 Hz), n.d. (*i*-PPh_3), 140.5 ($C^{5'}$), 142.3 (C^5), 154.0 ($C^{3'}$), 157.0 (C^3), 166.3 (CO_2^-), 179.7 (OAc-CO_2^-) ppm. ^{31}P NMR ($CDCl_3$, 161.8 MHz): δ = 53.4 ppm. Anal. Calcd for $C_{34}H_{36}N_5O_4PRu \times CH_2Cl_2$ (795.67): C, 52.83; H, 4.81; N, 8.80. Found: C, 52.90; H, 5.03; N, 8.89.

[Ru(bdmpza)(O_2CPh)(NCMe)(PPh_3)] (5b). Reaction of [Ru(bdmpza)(O_2CPh)(PPh_3)] (**2b**) (0.356 g, 0.487 mmol) in acetonitrile (25 mL) for 4 h according to method A afforded [Ru(bdmpza)(O_2CPh)(NCMe)(PPh_3)] (**5b**) as a yellow microcrystalline powder.

Yield 0.372 g (0.481 mmol, 99%). mp 160 °C (dec.). IR (CH_2Cl_2): $\tilde{\nu}$ = 2270 w (C≡N), 1663 vs (CO_2^-), 1645 sh, 1608 m, 1574 m (C=N), 1570 m, 1484 w, 1464 vw, 1434 m, 1419 vw cm^{-1}. IR (KBr): $\tilde{\nu}$ = 2268 m (C≡N), 1659 vs (CO_2^-), 1605 s, 1570 s (C=N), 1484 w, 1465 vw, 1434 m, 1419 vw cm^{-1}. UV/vis (CH_2Cl_2): λ_{max}/nm (log ε) = 238.0 (4.33), 268.0 (3.94), 275.0 (3.93), 296.0 (3.93). FAB-MS (NBOH-matrix): *m*/*z* (%) = 773 (3) [M^+], 731 (100) [M^+ − MeCN], 651 (29) [$M^+ - O_2CPh$], 610 (43) [$M^+ - O_2CPh$ − MeCN]. Isomer A: ^{1}H NMR ($CDCl_3$, 600 MHz): δ = 1.61 (s, 3H, C^3−CH_3), 2.23 (s, 3H, NC-CH_3), 2.30 (s, 3H, $C^{3'}$-CH_3), 2.51 (s, 3H, $C^{5'}$-CH_3), 2.57 (s, 3H, C^5−CH_3), 5.93 (s, 1H, H_{pz}), 6.01 (s, 1H, $H_{pz'}$), 6.62 (s, 1H, CH), 7.05−7.65 (m, 20H, Ph and PPh_3) ppm. ^{13}C NMR ($CDCl_3$, 150.9 MHz): δ = 2.23 (NC-CH_3), 11.0 ($C^{5'}$-CH_3), 11.6 (C^5−CH_3), 13.3 ($C^{3'}$-CH_3), 14.2 (C^3−CH_3), 69.6 (CH), 108.0 ($C^{4'}$), 108.4 (C^4), 124.7 (CN), 140.2 ($C^{5'}$), 142.4 (C^5), 153.8 ($C^{3'}$), 157.0 (C^3), 166.8 (CO_2^-), 174.6 (Ph-CO_2^-) ppm. ^{31}P NMR ($CDCl_3$, 161.8 MHz): δ = 53.6 ppm. Isomer B: ^{1}H NMR ($CDCl_3$, 600 MHz): δ = 1.57 (s, 3H, C^3−CH_3), 1.92 (s, 3H, NC-CH_3), 2.25 (s, 3H, $C^{3'}$-CH_3), 2.49 (s, 3H, $C^{5'}$-CH_3), 2.57 (s, 3H, C^5−CH_3), 5.91 (s, 1H, H_{pz}), 5.97 (s, 1H, $H_{pz'}$), 6.56 (s, 1H, CH), 7.05−7.65 (m, 20H, Ph and PPh_3) ppm. ^{13}C NMR ($CDCl_3$, 150.9 MHz): δ = 3.56 (NC-CH_3), 11.0 ($C^{5'}$-CH_3), 11.5 (C^5−CH_3), 13.2 ($C^{3'}$-CH_3), 13.9 (C^3−CH_3), 69.2 (CH), 107.8 ($C^{4'}$), 108.3 (C^4), 124.1 (CN), 140.2 ($C^{5'}$), 141.5 (C^5), 153.9 ($C^{3'}$), 157.5 (C^3), 167.8 (CO_2^-), 174.9 (Ph-CO_2^-) ppm. ^{31}P NMR ($CDCl_3$, 161.8 MHz): δ = 51.9 ppm. ^{13}C NMR (both isomers, $CDCl_3$, 150.9 MHz): δ = 126.2, 126.6, 126.9, 127.4, 127.6, 127.7, 127.9, 128.4, 128.5, 128.6, 128.7, 128.9, 129.0, 131.9, 132.0, 132.1, 133.6, 133.7, 134.0, 134.1, 134.4, 134.8, 135.0, 137.3, 137.7 (Ph and PPh_3). Anal. Calcd for $C_{39}H_{38}N_5O_4PRu$ (772.80): C, 60.61; H, 4.96; N, 9.06. Found C, 60.27; H, 5.07; N, 8.84.

Method B: General Procedure for the Syntheses of Pyridine Complexes. To a solution of the chlorido, carboxylato, or 2-oxocarboxylato complexes **1**, **2a**, **2b**, and **3a**−**c** in dichloromethane was added pyridine. The reaction mixture was stirred at ambient temperature and the progress of the reaction was monitored by IR spectroscopy. After the reaction was completed, the solvent was reduced in vacuo, and the product was precipitated with *n*-pentane. The precipitate was filtered off and dried in vacuo.

[Ru(bdmpza)Cl(PPh_3)(py)] (6). Reaction of [Ru(bdmpza)Cl(PPh_3)$_2$] (**1**) (0.308 g, 0.339 mmol) in CH_2Cl_2 (15 mL) with pyridine (0.271 g, 3.43 mmol) for 3 days according to method B afforded [Ru(bdmpza)Cl(PPh_3)(py)] (**6**) as a yellow crystalline powder.

Yield 0.237 g (0.327 mmol, 96%). mp 240 °C (dec.). IR (CH_2Cl_2): $\tilde{\nu}$ = 1659 vs (CO_2^-), 1565 w (C=N), 1482 m, 1462 vw, 1447 vw, 1434 m, 1420 vw cm^{-1}. IR (KBr): $\tilde{\nu}$ = 1657 vs (CO_2^-), 1642 vw, 1565 m (C=N), 1483 m, 1461 w, 1446 vw, 1437 w, 1432 w, 1419 vw cm^{-1}. UV/vis (CH_2Cl_2): λ_{max}/nm (log ε) = 235.0 (4.33), 268.0 (3.74), 275.0 (3.75), 304.0 (3.76), 362.0 (3.71). FAB-MS (NBOH-matrix): *m*/*z* (%) = 724 (7) [M^+], 647 (7) [M^+ − Py], 460 (6) [$M^+ - PPh_3$], 363 (6) [M^+ − Cl − Py − bdmpza], 217 (100) [$M^+ - PPh_3$ − bdmpza]. ^{1}H NMR ($CDCl_3$, 250 MHz): δ = 1.70 (s, 3H, $C^{3'}$-CH_3), 1.91 (s, 3H, C^3−CH_3), 2.48 (s, 3H, $C^{5'}$-CH_3), 2.52 (s, 3H, C^5−CH_3), 5.85 (s, 1H, H_{pz}), 5.92 (s, 1H, $H_{pz'}$), 6.52 (s, 1H, CH), 6.72 (t, 1H, *m*′-py), 6.87 (t, 1H, *m*-py), 7.12 (m, 6H, *m*-PPh_3), 7.17 (m, 6H, *o*-PPh_3), 7.23 (m, 3H, *p*-PPh_3), 7.36 (t, 1H, *p*-py), 8.02 (d 1H, *o*-py), 8.94 (d, 1H, *o*′-py) ppm. ^{13}C NMR ($CDCl_3$, 100.5 MHz): δ = 11.1 ($C^{5'}$-CH_3), 11.4 (C^5−CH_3), 12.6 ($C^{3'}$-CH_3), 14.9 (C^3−CH_3), 69.3 (CH), 108.9 (d, $C^{4'}$), 109.3 (C^4), 122.8, 122.9 (*m*- and *m*′-py), 127.4 (*m*-PPh_3), 128.7 (*p*-PPh_3), 134.1 (*p*-py), 134.1 (*o*-PPh_3), n.d. (*i*-PPh_3), 140.2 ($C^{5'}$), 141.6 (C^5), 154.6 ($C^{3'}$), 155.2 (*o*-py), 158.6 (*o*′-py), 158.8 (C^3), 168.1 (CO_2^-) ppm. ^{31}P NMR ($CDCl_3$, 161.8 MHz): δ = 49.5 ppm. Anal. Calcd for $C_{35}H_{35}ClN_5O_2PRu$ (725.19): C, 57.97; H, 4.86; N, 9.66. Found: C, 57.81; H, 4.99; N, 8.96.

[Ru(bdmpza)(O_2CMe)(PPh_3)(py)] (7a). Reaction of [Ru(bdmpza)(O_2CMe)(PPh_3)] (**2a**) (0.278 g, 0.415 mmol) in CH_2Cl_2 (10 mL) with pyridine (0.336 g, 4.25 mmol) for 3 days according to method B afforded [Ru(bdmpza)(O_2CMe)(PPh_3)(py)] (**7a**) as an orange microcrystalline powder.

Yield 0.266 g (0.355 mmol, 86%). mp 200 °C (dec.). IR (CH_2Cl_2): $\tilde{\nu}$ = 1659 vs (CO_2^-), 1619 s, 1567 w (C=N), 1482 m, 1464 vw, 1448 w, 1434 m, 1420 vw cm^{-1}. IR (KBr): $\tilde{\nu}$ = 1667 vs (CO_2^-), 1631 vs, 1565 w (C=N), 1481 m, 1465 vw, 1444 vw, 1434 w, 1420 vw cm^{-1}. UV/vis (CH_2Cl_2): λ_{max}/nm (log ε) = 237.0 (4.32), 268.0 (3.74), 274.0 (3.76), 311.0 (3.84), 368.0 (3.81). FAB-MS (NBOH-matrix): *m*/*z* (%) = 749 (29) [M^+], 689 (88) [$M^+ - O_2CMe$], 670 (100) [M^+ − Py], 611 (41) [$M^+ - O_2CMe$ − Py], 565 (29) [$M^+ - HO_2CMe - CO_2$ − Py − H], 363 (71) [$M^+ - O_2CMe$ − Py − bdmpza]. ^{1}H NMR ($CDCl_3$, 250 MHz): δ = 1.33 (s, 3H, $C^{3'}$-CH_3), 1.55 (s, 3H, C^3−CH_3), 1.79 (s, 3H, OAc-CH_3), 2.49 (s, 3H, $C^{5'}$-CH_3), 2.52 (s, 3H, C^5-CH_3), 5.79 (s, 1H, H_{pz}), 5.85 (s, 1H, $H_{pz'}$), 6.53 (s, 1H, CH), 6.82 (m, 2H, *m* and *m*′-py), 7.05−7.30 (m, 15H, PPh_3), 7.37 (tt, 1H, *p*-py), 8.05 (d, 1H, *o*-py), 8.90 (d, 1H, *o*′-py) ppm. ^{1}H NMR ($CDCl_3$, 400 MHz): δ = 1.32 (s, 3H, $C^{3'}$-CH_3), 1.59 (s, 3H, C^3-CH_3), 1.88 (br, 3H, OAc-CH_3), 2.52 (s, 3H, $C^{5'}$-CH_3), 2.59 (br, 3H, C^5-CH_3), 5.77 (s, 1H, H_{pz}), 5.83 (s, 1H, $H_{pz'}$), 6.55 (s, 1H, CH), 6.84 (br, 1H, *m*′-py), 6.85 (br, 1H, *m*-py), 7.11 (m, 6H, *m*-PPh_3), 7.17 (m, 6H, *o*-PPh_3), 7.23 (t, 3H, *p*-PPh_3), 7.34 (t, 1H, *p*-py), 7.97 (br, 1H, *o*-py), 8.93 (br, 1H, *o*′-py) ppm. ^{13}C NMR ($CDCl_3$, 62.9 MHz): δ = 11.2 ($C^{5'}$-CH_3), 11.5 ($C^{3'}$-CH_3), 11.5 (C^5−CH_3),14.2 (C^3−CH_3), 24.8 (OAc-CH_3), 69.3 (CH), 108.0 (d, $C^{4'}$, $^4J_{CP}$ = 2.8 Hz), 108.1 (C^4), 122.6 (*m*′-py), 123.2 (*m*-py), 127.4 (d, *m*-PPh_3, $^3J_{CP}$ = 8.9 Hz), 128.7 (*p*-PPh_3), 133.7 (*p*-py), 133.9 (d, *o*-PPh_3, $^2J_{CP}$ = 9.5 Hz), 135.0 (d, *i*-PPh_3, $^1J_{CP}$ = 38.2 Hz), 139.9 ($C^{5'}$), 141.1 (C^5), 153.9 (d, $C^{3'}$, $^3J_{CP}$ = 2.8 Hz), 154.6 (*o*-py), 155.5 (*o*′-py), 157.7 (C^3), 168.4 (CO_2^-),

178.0 (OAc-CO_2^-) ppm. ^{13}C NMR ($CDCl_3$, 100.5 MHz): δ = 11.2 ($C^{5'}$-CH_3), 11.5 ($C^{3'}$-CH_3), 11.5 (C^5-CH_3), 14.2 (C^3-CH_3), 24.8 (OAc-CH_3), 69.2 (CH), 107.9 (d, $C^{4'}$, $^4J_{CP}$ = 2.8 Hz), 108.1 (C^4), 122.6 (*m*′-py), 123.2 (*m*-py), 127.4 (d, *m*-PPh_3, $^3J_{CP}$ = 8.8 Hz), 128.7 (*p*-PPh_3), 133.7 (*p*-py), 133.9 (br, *o*-PPh_3), 134.9 (d, *i*-PPh_3, $^1J_{CP}$ = 38.3 Hz), 139.9 ($C^{5'}$), 141.1 (C^5), 153.9 (d, $C^{3'}$, $^3J_{CP}$ = 2.8 Hz), 154.4 (*o*-py), 155.4 (*o*′-py), 157.7 (C^3), 168.4 (CO_2^-), 178.1 (OAc-CO_2^-) ppm. ^{31}P NMR ($CDCl_3$, 161.8 MHz): δ = 49.7 ppm. Anal. Calcd $C_{37}H_{38}N_5O_4PRu$ (748.78): C, 59.35; H, 5.12; N, 9.35. Found: C, 59.28; H, 5.22; N, 9.31.

[Ru(bdmpza)(O_2CPh)(PPh_3)(py)] (7b). Reaction of [Ru(bdmpza)(O_2CPh)(PPh_3)] (**2b**) (0.261 g, 0.357 mmol) in CH_2Cl_2 (15 mL) with pyridine (0.270 g, 3.41 mmol) for 3 days according to method B afforded [Ru(bdmpza)(O_2CPh)(PPh_3)(py)] (**7b**) as yellow powder.

Yield 0.265 g (0.327 mmol, 92%). mp 220 °C (dec.). IR (CH_2Cl_2): $\tilde{\nu}$ = 1659 vs (CO_2^-), 1636 w, 1626 w, 1618 w, 1575 m (C=N), 1568 w, 1482 m, 1464 vw, 1447 w, 1434 w, 1420 vw cm^{-1}. IR (KBr): $\tilde{\nu}$ = 1662 vs (CO_2^-), 1641 vs, 1630 vs, 1623 s, 1573 m (C=N), 1561 m, 1483 s, 1465 w, 1450 w, 1444 vw, 1437 vw, 1433 w, 1419 vw cm^{-1}. UV/vis (CH_2Cl_2): λ_{max}/nm (log ε) = 235.0 (4.35), 268.0 (3.80), 274.0 (3.79), 315.0 (3.88), 361.0 (3.80). FAB-MS (NBOH-Matrix): *m*/*z* (%) = 810 (9) [M^+], 731 (100) [M^+ − Py], 690 (31) [M^+ − O_2Ph], 611 (17) [M^+ − O_2CPh − Py], 549 (60) [M^+ − PPh_3], 363 (34) [M^+ − O_2CPh − Py − bdmpza]. ^{1}H NMR ($CDCl_3$, 600 MHz): δ = 1.16 (s, 3H, $C^{3'}$-CH_3), 1.53 (s, 3H, C^3-CH_3), 2.52 (s, 3H, $C^{5'}$-CH_3), 2.60 (s, 3H, $C^{5'}$-CH_3), 5.75 (s, 1H, H_{pz}), 5.80 (s, 1H, $H_{pz'}$), 6.59 (s, 1H, CH), 6.91 (br, 2H, *m*-py), 7.10−7.50 (m, 20H, Ph and PPh_3), 7.98 (t, 1H, *p*-py), 8.05 (br, 1H, *o*-py), 9.12 (br, 1H, *o*′-py) ppm. ^{13}C NMR ($CDCl_3$, 150.9 MHz): δ = 11.2 (C^5-CH_3), 11.5 ($C^{3'}$-CH_3), 11.6 ($C^{5'}$-CH_3), 14.4 (C^3-CH_3), 69.3 (CH), 107.9 ($C^{4'}$), 108.1 (C^4), 122.7, 123.4 (*m* and *m*′-py), 127.3 (*m*-Ph), 127.5 (d, *m*-PPh_3, $^3J_{CP}$ = 7.8 Hz), 128.7 (*o*-Ph), 128.8 (*p*-PPh_3), 129.1 (*p*-Ph), 133.9 (br, *p*-py and *o*-PPh_3), 135.0 (d, *i*-PPh_3, $^1J_{CP}$ = 38.3 Hz), 137.1 (*i*-Ph), 139.7 ($C^{5'}$), 140.9 (C^5), 153.8 ($C^{3'}$), 154.8 (*o*-py), 155.5 (*o*′-py), 157.6 (C^3), 168.5 (CO_2^-), 171.1 (Ph-CO_2^-) ppm. ^{31}P NMR ($CDCl_3$, 161.8 MHz): δ = 50.5 ppm. For further purification yellow microystals of **7b** were obtained from a CH_2Cl_2 solution layered with a 1:1 mixture (v/v) of pentane/diethylether. According to the ^{1}H NMR spectrum these crystals contained also 1 equiv CH_2Cl_2. Anal. Calcd for $C_{42}H_{40}N_5O_4PRu$ × CH_2Cl_2 (895.79): C, 57.66; H, 4.73; N, 7.82. Found: C, 57.88; H, 4.75; N, 7.91.

[Ru(bdmpza)(O_2CC(O)Me)(PPh_3)(py)] (8a). Reaction of [Ru(bdmpza)(O_2CC(O)Me)(PPh_3)] (**3a**) (0.267 g, 0.383 mmol) in CH_2Cl_2 (15 mL) with pyridine (0.311 g, 3.93 mmol) for 3 days according to method B afforded [Ru(bdmpza)(O_2CC(O)Me)-(PPh_3)(py)] (**8a**) as an orange crystalline powder.

Yield 0.245 g (0.315 mmol, 82%). mp 175 °C (dec.). IR (CH_2Cl_2): $\tilde{\nu}$ = 1707 m, 1662 vs (CO_2^-), 1640 s, 1565 w (C=N), 1483 m, 1464 vw, 1448 w, 1434 m, 1421 w cm^{-1}. IR (KBr): $\tilde{\nu}$ = 1706 m, 1668 vs (CO_2^-), 1637 s, 1561 m (C=N), 1482 m, 1465 vw, 1446 w, 1436 w, 1420 w cm^{-1}. UV/vis (CH_2Cl_2): λ_{max}/nm (log ε) = 236.0 (4.36), 307.0 (3.86), 361.0 (3.81), 275.0 (3.78). FAB-MS (NBOH-matrix): *m*/*z* (%) = 776 (38) [M^+], 689 (50) [M^+ − O_2CC(O)Me], 611 (56) [M^+ − O_2CC(O)Me − Py], 515 (25) [M^+ − PPh_3], 363 (100) [M^+ − O_2CC(O)Me − Py − bdmpza]. ^{1}H NMR ($CDCl_3$, 250 MHz): δ = 1.26, 1.47 (s, 3H, C^3 and $C^{3'}$-CH_3), 2.18 (s, 3H, C(O)-CH_3), 2.49, 2.53 (s, 3H, C^5 or $C^{5'}$-CH_3), 5.80, 5.85 (s, 1H, H_{pz} and $H_{pz'}$), 6.55 (s, 1H, CH), 6.84 (m, 2H, *m*- and *m*′-py), 7.05−7.30 (m, 15H, PPh_3), 7.38 (t, 1H, *p*-py), 8.05, 8.93 (d, 1H, *o*- and *o*′-py) ppm. ^{13}C NMR ($CDCl_3$, 100.5 MHz): δ = 11.2, 11.5, 11.5, 14.1 (C^3, $C^{3'}$, C^5 and $C^{5'}$-CH_3), 26.6 (C(O)-CH_3), 69.3 (CH), 108.1, 108.2 (C^4 or $C^{4'}$), 123.0, 123.4 (*m*- and *m*′-py), 127.6 (d, *m*-PPh_3, $^3J_{CP}$ = 9.0 Hz), 128.8 (*p*-PPh_3), 133.9 (d, *o*-PPh_3, $^2J_{CP}$ = 10.2 Hz), 134.0 (*p*-py), 134.6 (d, *i*-PPh_3, $^1J_{CP}$ = 38.9 Hz), 140.1, 141.4 (C^5 and $C^{5'}$), 154.0 (C^3 and $C^{3'}$), 154.4, 155.5 (*o* and *o*′-py), 157.7 (C^3 and $C^{3'}$), 168.4 (CO_2^-), 171.1 (C(O)-CO_2^-), 197.6 (C=O) ppm. ^{31}P NMR ($CDCl_3$, 161.8 MHz): δ = 49.7 ppm. Anal. Calcd for $C_{38}H_{35}N_5O_5PRu$ (776.79): C, 58.76; H, 4.93; N, 9.02. Found: C, 58.42; H, 5.20; N, 8.76.

[Ru(bdmpza)(O_2CC(O)Et)(PPh_3)(py)] (8b). Reaction of [Ru(bdmpza)(O_2CC(O)Et)(PPh_3)] (**3b**) (0.269 g, 0.378 mmol) in CH_2Cl_2 (15 mL) with pyridine (0.302 g, 3.82 mmol) for 3 days according to method B afforded [Ru(bdmpza)(O_2CC(O)Et)-(PPh_3)(py)] (**8b**) as an orange crystalline powder. Crystals suitable for X-ray structure determination were obtained from a CH_2Cl_2 solution layered with *n*-hexane.

Yield 0.209 g (0.264 mmol, 70%). mp 210 °C (dec.). IR (CH_2Cl_2): $\tilde{\nu}$ = 1711 w, 1661 vs (CO_2^-), 1640 s, 1565 w (C=N), 1483 m, 1463 vw, 1448 w, 1434 m, 1420 vw cm^{-1}. IR (KBr): $\tilde{\nu}$ = 1709 m, 1664 vs (CO_2^-), 1639 vs, 1565 m (C=N), 1482 m, 1464 vw, 1448 w, 1437 w, 1433 w, 1420 vw cm^{-1}. UV/vis (CH_2Cl_2): λ_{max}/nm (log ε) = 236.0 (4.34), 268.0 (3.77), 275.0 (3.79), 307.0 (3.85), 362.0 (3.80). FAB-MS (NBOH-matrix): *m*/*z* (%) = 791 (33) [M^+], 711 (14) [M^+ − Py], 689 (100) [M^+ − O_2CC(O)Et], 611 (43) [M^+ − O_2CC(O)Et − Py], 529 (14) [M^+ − PPh_3], 363 (48) [M^+ − O_2CC(O)Et − Py − bdmpza]. ^{1}H NMR ($CDCl_3$, 400 MHz): δ = 1.02 (t, 3H, CH_2−CH_3, $^3J_{HH}$ = 7.3 Hz), 1.26 (s, 3H, $C^{3'}$-CH_3), 1.48 (s, 3H, C^3-CH_3), 2.48 (s, 3H, $C^{5'}$-CH_3), 2.52 (s, 3H, C^5-CH_3), 2.58 (q, 2H, CH_2−CH_3, $^3J_{HH}$ = 7.3 Hz), 5.80 (s, 1H, H_{pz}), 5.85 (s, 1H, $H_{pz'}$), 6.55 (s, 1H, CH), 6.83 (m, 2H, *m*- and *m*′-py), 7.05−7.30 (m, 15H, PPh_3), 7.36 (t, 1H, *p*-py), 8.05 (d, 1H, *o*-py), 8.96 (d, 1H, *o*′-py) ppm. ^{13}C NMR ($CDCl_3$, 100.5 MHz): δ = 7.45 (CH_2−CH_3), 11.2 ($C^{5'}$-CH_3), 11.5 (C^5-CH_3), 11.6 ($C^{3'}$-CH_3), 14.1 (C^3-CH_3), 32.0 (CH_2), 69.2 (CH), 108.0 (d, $C^{4'}$, $^4J_{CP}$ = 2.8 Hz), 108.2 (C^4), 123.0, 123.3 (*m*- and *m*′-py), 127.5 (d, *m*-PPh_3, $^3J_{CP}$ = 9.0 Hz), 128.8 (*p*-PPh_3), 134.0 (*p*-py), 133.9 (d, *o*-PPh_3, $^2J_{CP}$ = 8.8 Hz), 134.6 (d, *i*-PPh_3, $^1J_{CP}$ = 39.1 Hz), 140.1 ($C^{5'}$), 141.4 (C^5), 153.9 (d, $C^{3'}$, $^3J_{CP}$ = 2.4 Hz), 154.3 (*o*-py), 155.5 (*o*′-py), 157.7 (C^3), 168.4 (CO_2^-), 171.6 (C(O)-CO_2^-), 200.3 (C=O) ppm. ^{31}P NMR ($CDCl_3$, 161.8 MHz): δ = 49.8 ppm. Anal. Calcd for $C_{39}H_{40}N_5O_5PRu$ (790.82): C, 59.23; H, 5.10; N, 8.86. Found: C, 58.62; H, 5.31; N, 8.75.

[Ru(bdmpza)(O_2C(CO)Ph)(PPh_3)(py)] (8c). Reaction of [Ru(bdmpza)(O_2CC(O)Ph)(PPh_3)] (**3c**) (0.300 g, 0.395 mmol) in CH_2Cl_2 (15 mL) with pyridine (0.314 g, 3.97 mmol) for 3 days according to method B afforded [Ru(bdmpza)(O_2CC(O)Ph)-(PPh_3)(py)] (**8c**) as an orange crystalline powder.

Yield 0.224 g (0.267 mmol, 68%). mp 205 °C (dec.). IR (CH_2Cl_2): $\tilde{\nu}$ = 1662 vs (CO_2^-), 1634 s, 1597 vw, 1565 w (C=N), 1483 m, 1463 vw, 1448 w, 1434 w, 1421 vw cm^{-1}. IR (KBr): $\tilde{\nu}$ = 1665 vs (CO_2^-), 1640 vs, 1598 vw, 1564 m (C=N), 1482 m, 1464 vw, 1447 w, 1436 vw, 1433 w, 1420 vw cm^{-1}. UV/vis (CH_2Cl_2): λ_{max}/nm (log ε) = 236.0 (4.44), 362.0 (3.76). FAB-MS (NBOH-matrix): *m*/*z* (%) = 839 (26) [M^+], 759 (26) [M^+ − Py], 690 (54) [M^+ − O_2CC(O)Ph], 611 (100) [M^+ − O_2CC(O)Ph − Py], 567 (43) [M^+ − PPh_3], 363 (71) [M^+ − O_2CC(O)Ph − Py − bdmpza]. ^{1}H NMR ($CDCl_3$, 400 MHz): δ = 1.40 (s, 3H, $C^{3'}$-CH_3), 1.63 (s, 3H, C^3-CH_3), 2.51 (s, 3H, $C^{5'}$-CH_3), 2.55 (s, 3H, C^5-CH_3), 5.84 (s, 1H, H_{pz}), 5.90 (s, 1H, $H_{pz'}$), 6.57 (s, 1H, CH), 6.82 (m, 1H, *m*′-py), 6.86 (m, 1H, *m*-py), 7.04 (m, 6H, *m*-PPh_3), 7.10 (m, 3H, *p*-PPh_3), 7.20 (m, 6H, *o*-PPh_3), 7.34 (m, 2H, *m*-Ph), 7.37 (m, 1H, *p*-py), 7.50 (m, 1H, *p*-Ph), 8.02 (m, 2H, *o*-Ph), 8.05 (d, 1H, *o*-py), 8.90 (d, 1H, *o*′-py) ppm. ^{13}C NMR ($CDCl_3$, 100.5 MHz): δ = 11.2 ($C^{5'}$-CH_3), 11.6 (C^5-CH_3), 12.0 (C^3-CH_3), 14.6 ($C^{3'}$-CH_3), 69.2 (CH), 108.2 (d, $C^{4'}$, $^4J_{CP}$ = 2.7 Hz), 108.3 (C^4), 123.0 (*m*′-py), 123.4 (*m*-

py), 127.5 (d, *m*-PPh_3, $^3J_{CP}$ = 8.9 Hz), 128.1 (*p*-Ph), 128.8 (*p*-PPh_3), 130.0 (*o*-Ph), 132.7 (*i*-Ph), 133.9 (d, *o*-PPh_3, $^2J_{CP}$ = 9.1 Hz), 134.1 (*p*-py), 134.4 (*p*-Ph), 134.5 (d, *i*-PPh_3, $^1J_{CP}$ = 39.1 Hz), 140.2 ($C^{5'}$), 141.5 (C^5), 154.3 ($C^{3'}$), 154.3 (*o*-py), 155.6 (*o*′-py), 157.8 (C^3), 168.4 (CO_2^-), 172.5 (C(O)-CO_2^-), 190.4 (C=O) ppm. ^{31}P NMR ($CDCl_3$, 161.8 MHz): δ = 49.8 ppm. Anal. Calcd for $C_{43}H_{40}N_5O_5PRu$ (838.86): C, 61.57; H, 4.81; N, 8.35. Found: C, 61.37; H, 4.89; N, 8.40.

Method C: General Procedure for Complex Syntheses with Gaseous CO, SO_2, and NO. A solution of the acetato, benzoato, or benzoylformato complexes **2a**, **2b**, or **3c** in dichloromethane was flushed with gaseous CO, SO_2, or NO under stirring at ambient temperature. The progress of the reactions was monitored by IR spectroscopy. After the reaction was completed, the solvent was reduced in vacuo, and the product was precipitated with *n*-pentane. The precipitate was filtered off and dried in vacuo.

[Ru(bdmpza)(O_2CMe)(CO)(PPh_3)] (9a). Reaction of [Ru(bdmpza)(O_2CMe)(PPh_3)] (**2a**) (275 mg, 0.411 mmol) in CH_2Cl_2 (100 mL) with CO for 2 h according to method C afforded the product [Ru(bdmpza)(O_2CMe)(CO)(PPh_3)] (**9a**) as a yellow powder.

Yield 325 mg (0.400 mmol, 97%). mp 150 °C (dec.). IR (CH_2Cl_2): $\tilde{\nu}$ = 1977 vs (CO), 1669 vs (CO_2^-), 1624 w, 1602 vw, 1564 w (C=N), 1485 vw, 1465 vw, 1437 m, 1419 vw cm^{-1}. IR (KBr): $\tilde{\nu}$ = 1967 vs (CO), 1672 vs (CO_2^-), 1620 m, 1600 vw, 1560 m (C=N), 1481 vw, 1462 vw, 1434 m, 1420 vw cm^{-1}. UV/vis (CH_2Cl_2): λ_{max} (log ε) = 245.0 (4.17). FAB MS (NBOH): *m*/*z* (%) = 698 (34) [M^+], 639 (100) [$M^+ - O_2$CMe], 565 (12) [$M^+ - HO_2$CMe $- CO_2 - CO - H$], 391 (41) [M^+ − bdmpzaH − O_2CMe], 363 (35) [M^+ − bdmpzaH − O_2CMe − CO]. ^{1}H NMR (CD_2Cl_2, 600 MHz): δ = 1.55 (s, 3H, OAc-CH_3), 1.91 (s, 3H, C^3-CH_3), 2.33 (s, 3H, $C^{3'}$-CH_3), 2.46 (s, 3H, $C^{5'}$-CH_3), 2.55 (s, 3H, C^5-CH_3), 6.03 (s, 1H, H_{pz}), 6.04 (s, 1H, $H_{pz'}$), 6.57 (s, 1H, CH), 7.32 (vt, 6, m-PPh_3), 7.40 (vt, 9, *o*- and *p*-PPh_3). ^{13}C NMR (CD_2Cl_2, 150.9 MHz): δ = 11.3 ($C^{5'}$-CH_3), 11.5 (C^5-CH_3), 13.7 (C^3-CH_3), 14.0 ($C^{3'}$-CH_3), 22.9 (OAc-CH_3), 69.3 (CH), 108.6 ($C^{4'}$), 109.3 (C^4), 128.4 (d, *m*-PPh_3, $^3J_{CP}$ = 9.8 Hz), 130.4 (d, *p*-PPh_3), 133.1 (d, *i*-PPh_3, $^1J_{CP}$ = 46.4 Hz), 134.0 (d, *o*-PPh_3, $^2J_{CP}$ = 9.9 Hz), 142.1 ($C^{5'}$), 142.9 (C^5), 154.6 ($C^{3'}$), 155.9 (C^3), 166.3 (CO_2^-), 177.3 (OAc-CO_2^-), 205.3 (d, CO, $^2J_{CP}$ = 19.8 Hz). ^{31}P NMR ($CDCl_3$, 161.8 MHz): δ = 43.3. Anal. Calcd for $C_{33}H_{33}N_4O_5PRu$ (697.69): C, 56.81; H, 4.77; N, 8.03. Found: C, 57.25; H, 4.86; N, 7.91.

[Ru(bdmpza)(O_2CPh)(CO)(PPh_3)] (9b). Reaction of [Ru(bdmpza)(O_2CPh)(PPh_3)] (**2b**) (341 mg, 0.466 mmol) in CH_2Cl_2 (100 mL) with CO for 1 h according to method C afforded [Ru(bdmpza)(O_2CPh)(CO)(PPh_3)] (**9b**) as a yellow powder.

Yield 323 mg (0.425 mmol, 91%). mp 170 °C (dec.). IR (CH_2Cl_2): $\tilde{\nu}$ = 1978 vs (CO), 1669 vs (CO_2^-), 1636 w, 1616 w, 1576 w, 1564 w (C=N), 1485 vw, 1465 vw, 1447 vw, 1436 m, 1419 vw cm^{-1}. IR (KBr): $\tilde{\nu}$ = 1953 vs (CO), 1670 vs (CO_2^-), 1636 w, 1617 w, 1576 vw, 1565 w (C=N), 1481 vw, 1463 vw, 1446 vw, 1437 m, 1432 m, 1420 vw cm^{-1}. UV/vis (CH_2Cl_2): λ_{max} (log ε) = 246.0 (4.21). FAB MS (NBOH): *m*/*z* (%) = 760 (49) [M^+], 732 (25) [$M^+ - CO$], 638 (100) [$M^+ - HO_2$CPh], 565 (11) [$M^+ - HO_2$CPh $- CO_2 - CO - H$], 363 (23) [M^+ − bdmpzaH − O_2CPh − CO]. ^{1}H NMR ($CDCl_3$, 400 MHz): δ = 1.95 (s, 3H, C^3-CH_3), 2.24 (s, 3H, $C^{3'}$-CH_3), 2.45 (s, 3H, $C^{5'}$-CH_3), 2.56 (s, 3H, C^5-CH_3), 5.94 (s, 1H, $H_{pz'}$), 6.02 (s, 1H, H_{pz}), 6.58 (s, 1H, CH), 7.10−7.20 (m, 8H, *m*-Ph and *m*-PPh_3), 7.23 (d, 1H, *p*-Ph), 7.29 (vt, 3H, *p*-PPh_3), 7.44 (vt, 6H, *o*-PPh_3), 7.55 (d, 2H, *o*-Ph). ^{13}C NMR ($CDCl_3$, 100.5 MHz): δ = 11.1 ($C^{5'}$-CH_3), 11.3 (C^5-CH_3), 13.8 ($C^{3'}$-CH_3), 13.9 (C^3-CH_3), 68.9 (CH), 108.3 (d, $C^{4'}$, $^4J_{CP}$ = 2.6 Hz), 108.8 (C^4), 127.0 (*m*-Ph), 128.1 (d, *m*-PPh_3, $^3J_{CP}$ = 9.9 Hz), 129.2 (*o*-Ph), 129.4 (*p*-Ph), 129.8 (d, *p*-PPh_3, $^4J_{CP}$ = 2.2 Hz), 132.6 (d, *i*-PPh_3, $^1J_{CP}$ = 46.9 Hz), 133.7 (d, *o*-PPh_3, $^2J_{CP}$ = 10.0 Hz), 135.4 (*i*-Ph), 140.9 ($C^{5'}$), 141.7 (C^5), 154.5 ($C^{3'}$), 155.4 (C^3), 166.3 (CO_2^-), 172.6 (Ph-CO_2^-), 204.2 (d, CO, $^2J_{CP}$ = 21.2 Hz). ^{31}P NMR ($CDCl_3$, 161.8 MHz): δ = 43.6. Anal. Calcd for $C_{38}H_{35}N_4O_5PRu$ (759.76): C, 60.07; H, 4.64; N, 7.37. Found: C, 59.98; H, 4.79; N, 7.32.

[Ru(bdmpza)(O_2CMe)(PPh_3)(SO_2)] (10a). Reaction of [Ru(bdmpza)(O_2CMe)(PPh_3)] (**2a**) (654 mg, 0.977 mmol) in CH_2Cl_2 (150 mL) with gaseous SO_2 for 30 min according to method C afforded [Ru(bdmpza)(O_2CMe)(SO_2)(PPh_3)] (**10a**) as a yellow powder.

Yield 678 mg (0.924 mmol, 95%). mp 180 °C (dec.). IR (CH_2Cl_2): $\tilde{\nu}$ = 1673 vs (CO_2^-), 1566 w (C=N), 1483 vw, 1465 vw, 1436 m, 1419 vw, 1395 vw, 1350 vw, 1313 vw, 1284 m, 1128 s, 1094 w, 1091 vw cm^{-1}. IR (KBr): $\tilde{\nu}$ = 1672 vs (CO_2^-), 1566 w (C=N), 1484 vw, 1463 vw, 1437 m, 1420 w, 1374 vw, 1352 vw, 1310 vw, 1282 m, 1128 s, 1093 w, 1089 vw cm^{-1}. UV/vis (CH_2Cl_2): λ_{max} (log ε) = 246.0 (4.26). FAB MS (NBOH): *m*/*z* (%) = 735 (30) [M^+ + H], 670 (100) [$M^+ - SO_2$], 611 (92) [$M^+ - SO_2 - O_2$CMe], 565 (27) [$M^+ - SO_2 - CO_2 - HO_2$CMe − H], 363 (20) [M^+ − bdmpzaH − SO_2 − O_2CMe]. ^{1}H NMR ($CDCl_3$, 250 MHz): δ = 1.77, 1.92, 2.12, 2.43, 2.48 (s, 15H, $C^{3,3',5,5'}$-CH_3, OAc-CH_3), 5.79, 5.92 (s, 2H, H_{pz} and $H_{pz'}$), 6.54 (s, 1H, CH), 7.00−7.65 (m, 15H, PPh_3). ^{13}C NMR ($CDCl_3$, 100.5 MHz): δ = 11.5 ($C^{5'}$-CH_3), 11.6 (C^5-CH_3), 13.7 ($C^{3'}$-CH_3), 14.0 (C^3-CH_3), 22.8 (OAc-CH_3), 69.3 (CH), 109.3 (C^4), 109.7 (d, $C^{4'}$, $^4J_{CP}$ = 2.7 Hz), 127.9 (d, *m*-PPh_3, $^3J_{CP}$ = 7.1 Hz), 129.7 (d, *p*-PPh_3), 134.8 (d, *o*-PPh_3, $^1J_{CP}$ = 9.4 Hz), n.d. (*i*-PPh_3), 141.1 (d, $C^{5'}$, $^5J_{CP}$ = 1.3 Hz), 142.8 (C^5), 155.0 (d, $C^{3'}$, $^3J_{CP}$ = 2.2 Hz), 156.4 (C^3), 167.0 (CO_2^-), 179.7 (OAc-CO_2^-). ^{31}P NMR ($CDCl_3$, 161.8 MHz): δ = 45.4. Anal. Calcd for $C_{32}H_{33}N_4O_6PRuS$ (733.74): C, 52.38; H, 4.53; N, 7.64. Found: C, 52.41; H, 4.70; N, 7.73.

[Ru(bdmpza)(O_2CPh)(PPh_3)(SO_2)] (10b). Reaction of [Ru(bdmpza)(O_2CPh)(PPh_3)] (**2b**) (638 mg, 0.872 mmol) in CH_2Cl_2 (80 mL) with gaseous SO_2 for 2 h according to method C afforded [Ru(bdmpza)(O_2CPh)(SO_2)(PPh_3)] (**10b**) as a yellow powder.

Yield 642 mg (0.807 mmol, 92%). mp 180 °C (dec.). IR (CH_2Cl_2): $\tilde{\nu}$ = 1673 vs (CO_2^-), 1567 w (C=N), 1507 w, 1484 vw, 1464 vw, 1435 w, 1420 vw, 1395 m, 1349 vw, 1313 vw, 1286 w, 1129 s, 1094 w, 1090 vw cm^{-1}. IR (KBr): $\tilde{\nu}$ = 1671 vs (CO_2^-), 1561 w (C=N), 1509 w, 1484 vw, 1461 vw, 1435 w, 1416 vw, 1397 m, 1346 vw, 1283 m, 1125 s, 1093 w cm^{-1}. UV/vis (CH_2Cl_2): λ_{max}/nm (log ε) = 247.0 (4.39). FAB MS (NBOH): *m*/*z* (%) = 797 (28) [M^+ + H], 732 (100) [$M^+ - SO_2$], 611 (93) [$M^+ - SO_2 - O_2$CPh], 566 (19) [$M^+ - SO_2 - CO_2$ − HOAc]. ^{1}H NMR (CD_2Cl_2, 600 MHz): δ = 1.98 (s, 3H, $C^{3'}$-CH_3), 2.02 (s, 3H, C^3-CH_3), 2.45 (s, 3H, $C^{5'}$-CH_3), 2.52 (s, 3H, C^5-CH_3), 5.88 (s, 1H, H_{pz}), 5.93 (s, 1H, $H_{pz'}$), 6.57 (s, 1H, CH), 7.19 (m, 6H, *m*-PPh_3), 7.33 (m, 5H, *p*-PPh_3, *m*-Ph), 7.39 (m, 6H, *o*-PPh_3), 7.48 (m, 1H, *p*-Ph), 7.64 (d, 2H, *o*-Ph). ^{13}C NMR (CD_2Cl_2, 150.9 MHz): δ = 11.5 ($C^{5'}$-CH_3), 11.4 (C6-CH_3), 13.4 ($C^{3'}$-CH_3), 14.2 (C^3-CH_3), 69.4 (CH), 109.4 (C^4), 109.6 ($C^{4'}$), 127.9 (d, $^3J_{CP}$ = 9.7 Hz, *m*-PPh_3), 128.4 (*p*-PPh_3), 129.8 (broad, *i*-PPh_3), 130.2 (*o*- and *m*-Ph), 132.7 (*p*-Ph), 134.8 (d, *o*-PPh_3, $^2J_{CP}$ = 9.2 Hz), 142.0 (d, $C^{5'}$), 143.6 (C^5), 155.2 (d, $C^{3'}$), 156.6 (C^3), 166.8 (CO_2^-), 175.4 (Ph-CO_2^-). ^{31}P NMR ($CDCl_3$, 161.8 MHz): δ = 44.6. Anal. Calcd for $C_{37}H_{35}N_4O_6PRuS$ (795.82): C, 55.84; H, 4.43; N, 7.04. Found: C, 55.49; H, 4.49; N, 6.73.

[Ru(bdmpza)(O_2CC(O)Ph)(NO)(PPh_3)]$^+$ (12). Reaction of [Ru(bdmpza)(O_2CC(O)Ph)(PPh_3)] (**3c**) (828 mg, 1.09 mmol) in THF (80 mL) with gaseous NO for 1.5 h according to method C afforded, after precipitation with diethylether, the product [Ru(bdmpza)(O_2CC(O)Ph)(NO)(PPh_3)]$^+$ (**12**) as a pale red solid.

Yield 848 mg. mp 55−60 °C (dec.). IR (CH_2Cl_2): $\tilde{\nu}$ = 1911 vs (NO), 1698 s, 1645 m, 1597 vw, 1562 w (C=N), 1483 w, 1463 vw, 1450 vw, 1439 m, 1436 m, 1418 vw cm^{-1}. IR (KBr): $\tilde{\nu}$ = 1906 vs (NO), 1688 vs (CO_2^-), 1662 s (CO_2^-), 1596 vw, 1561 m (C=N), 1482 vw, 1465 vw, 1437 m, 1420 vw cm^{-1}. UV/vis (CH_2Cl_2): λ_{max}/nm = 237.0, 268.0. FAB MS (NBOH): *m*/*z* (%) = 791 (100) [M^+], 641 (40) [$M^+ - O_2CC(O)Ph$], 363 (17) [M^+ − bdmpza − $O_2CC(O)Ph$ − NO]. ^1H NMR ($CDCl_3$, 250 MHz): δ = 1.95, 2.36, 2.57, 2.62 (s, 12H, $C^{3,3',5,5'}$-CH_3), 6.22, 6.24 (s, 2H, $H_{pz,pz'}$), 6.71 (s, 1H, CH), 7.30−7.70 (m, 18H, Ph and PPh_3), 7.99 (vt, 2H, *o*-Ph). ^{13}C NMR ($CDCl_3$, 62.9 MHz): δ = 11.1, 11.5, 13.9, 14.3 ($C^{3,3',5,5'}$-CH_3), 68.2 (CH), 110.1 (d, C^4 or $C^{4'}$, $^4J_{CP}$ = 3.2 Hz), 111.5 (C^4 or $C^{4'}$), 124.8 (d, *i*-PPh_3, $^1J_{CP}$ = 54.5 Hz), 128.9, 129.8 (d, *m*-PPh_3, $^3J_{CP}$ = 11.3 Hz), 129.9, 133.1, 133.2, 133.6 (d, *o*-PPh_3, $^2J_{CP}$ = 9.8 Hz), 134.7, 145.3 (d, C^5 or $C^{5'}$, $^5J_{CP}$ = 1.3 Hz), 146.8 (C^5 or $C^{5'}$), 154.3 (d, C^3 or $C^{3'}$, $^3J_{CP}$ = 2.2 Hz), 158.3 (C^3 or $C^{3'}$), 163.0 (CO_2^-), 169.4 (CO_2^-), 186.7 (C=O). ^{31}P NMR ($CDCl_3$, 161.8 MHz): δ = 24.2. Counterion unspecified.

Method D: General Procedure for the Syntheses of NO Complexes from [NO]BF_4. A solution of the carboxylato or 2-oxocarboxylato complexes **2a**, **2b**, or **3a**−**c** in dichloromethane was reacted with [NO]BF_4. After 0.5 to 1 h the reaction was completed, the solvent was reduced in vacuo, and the product was precipitated with diethylether. The precipitate was filtered off and dried in vacuo.

[Ru(bdmpza)(O_2CMe)(NO)(PPh_3)]BF_4 (13a). Reaction of [Ru(bdmpza)(O_2CMe)(PPh_3)] (**2a**) (533 mg, 0.796 mmol) with [NO]BF_4 (175 mg, 1.50 mmol) in CH_2Cl_2 (40 mL) at ambient temperature afforded after 30 min according to method D the product [Ru(bdmpza)(O_2CMe)(NO)(PPh_3)]BF_4 (**13a**) as a pale red powder.

Yield 593 mg (0.754 mmol, 95%). mp 175 °C (dec.). IR (CH_2Cl_2): $\tilde{\nu}$ = 1912 vs (NO), 1698 s (CO_2^-), 1635 m (CO_2^-), 1612 vw, 1562 m (C=N), 1483 w, 1465 w, 1439 m, 1415 vw cm^{-1}. IR (KBr): $\tilde{\nu}$ = 1897 vs (N−O), 1690 vs (CO_2^-), 1637 m (CO_2^-), 1612 vw, 1561 m (C=N), 1483 w, 1462 w, 1438 m, 1420 vw cm^{-1}. UV/vis (CH_2Cl_2): λ_{max}/nm (log ε) = 237.0 (4.32), 273.0 (4.31). FAB MS (NBOH): *m*/*z* (%) = 700 (100) [M^+], 641 (33) [$M^+ - O_2CMe$]. ^1H NMR ($CDCl_3$, 250 MHz): δ = 1.94 (s, 3H, C^3−CH_3), 2.07 (s, 3H, OAc-CH_3), 2.24 (s, 3H, $C^{3'}$-CH_3), 2.55 (s, 3H, $C^{5'}$-CH_3), 2.63 (s, 3H, C^5-CH_3), 6.23 (s, 1H, $H_{pz'}$), 6.46 (s, 1H, H_{pz}), 6.63 (s, 1H, CH), 7.36 (m, 6H, *o*-PPh_3), 7.50 (m, 6H, *m*-PPh_3), 7.63 (m, 3H, *p*-PPh_3). ^{13}C NMR ($CDCl_3$, 62.9 MHz): δ = 11.0 ($C^{5'}$-CH_3), 11.4 (C^5-CH_3), 13.2 ($C^{3'}$-CH_3), 14.1 (C^3-CH_3), 22.1 (OAc-CH_3), 68.2 (CH), 110.1 (d, $C^{4'}$, $^4J_{CP}$ = 2.9 Hz), 111.8 (C^4), 125.0 (d, *i*-PPh_3, $^1J_{CP}$ = 54.1 Hz), 129.6 (d, *m*-PPh_3, $^3J_{CP}$ = 10.8 Hz), 133.1 (*p*-PPh_3), 133.4 (d, *o*-PPh_3, $^2J_{CP}$ = 9.8 Hz), 145.0 (d, $C^{5'}$, $^5J_{CP}$ = 1.7 Hz), 146.7 (C^5), 154.2 (d, $C^{3'}$, $^3J_{CP}$ = 2.0 Hz), 158.2 (C^3), 163.3 (CO_2^-), 176.8 (OAc-CO_2^-). ^{31}P NMR ($CDCl_3$, 161.8 MHz): δ = 23.5. Anal. Calcd for $C_{32}H_{33}BF_4N_5O_5PRu$ (786.49): C, 48.87; H, 4.23; N, 8.90. Found: C, 48.45; H, 4.22; N, 8.99.

[Ru(bdmpza)(O_2CPh)(NO)(PPh_3)]BF_4 (13b). Reaction of [Ru(bdmpza)(O_2CPh)(PPh_3)] (**2b**) (355 mg, 0.485 mmol) with [NO]BF_4 (107 mg, 0.916 mmol) in CH_2Cl_2 (30 mL) for 1 h according to method D afforded [Ru(bdmpza)(O_2CPh)(NO)-(PPh_3)]BF_4 (**13b**) as a pale red powder.

Yield 390 mg (0.460 mmol, 95%). mp 130 °C (dec). IR (CH_2Cl_2): $\tilde{\nu}$ = 1912 vs (NO), 1696 s (CO_2^-), 1635 w (CO_2^-), 1616 vw, 1561 m (C=N), 1483 w, 1465 w, 1450 vw, 1437 m, 1420 vw cm^{-1}. IR (KBr): $\tilde{\nu}$ = 1903 vs (NO), 1692 vs (CO_2^-), 1632 w (CO_2^-), 1562 m (C=N), 1483 w, 1467 w, 1463 w, 1450 vw, 1439 m, 1435 m, 1416 vw cm^{-1}. UV/vis (CH_2Cl_2): λ_{max}/nm (log ε) = 239.0 (4.45), 273.0 (4.29). FAB MS (NBOH): *m*/*z* (%) = 763 (100) [M^+ + H], 733 (11) [M^+ + H − NO], 641 (19) [$M^+ - O_2CPh$]. ^1H NMR ($CDCl_3$, 250 MHz): δ = 1.99 (s, 3H, C^3-CH_3), 2.13 (s, 3H, $C^{3'}$-CH_3), 2.59 (s, 3H, $C^{5'}$-CH_3), 2.70 (s, 3H, C^5-CH_3), 6.19 (s, 1H, $H_{pz'}$), 6.46 (s, 1H, H_{pz}), 6.76 (s, 1H, CH), 7.30−7.80 (m, 18H, Ph and PPh_3), 7.85 (d, 2H, *o*-Ph). ^{13}C NMR ($CDCl_3$, 100 MHz): δ = 11.0 ($C^{5'}$-CH_3), 11.5 (C^5-CH_3), 13.0 ($C^{3'}$-CH_3), 14.1 (C^3-CH_3), 68.2 (CH), 110.2 (d, $C^{4'}$, $^4J_{CP}$ = 3.1 Hz), 111.5 (C^4), 125.1 (d, *i*-PPh_3, $^1J_{CP}$ = 54.7 Hz), 128.5 (*p*-PPh_3), 129.5 (d, *m*-PPh_3, $^3J_{CP}$ = 11.4 Hz), 129.7 (*o*-Ph), 132.2 (*i*-Ph), 133.0 (*m*-Ph), 133.5 (d, *o*-PPh_3, $^2J_{CP}$ = 9.7 Hz), 134.0 (*p*-Ph), 145.1 (d, $C^{5'}$, $^5J_{CP}$ = 2.0 Hz), 146.9 (C^5), 154.2 (d, $C^{3'}$, $^3J_{CP}$ = 2.0 Hz), 157.6 (C^3), 163.6 (CO_2^-), 172.6 (Ph-CO_2^-). ^{31}P NMR ($CDCl_3$, 161.8 MHz): δ = 23.3. Anal. Calcd for $C_{37}H_{35}BF_4N_5O_5PRu$ (848.56): C, 52.37; H, 4.16; N, 8.25. Found: C, 51.94; H, 4.28; N, 8.35.

[Ru(bdmpza)($O_2CC(O)Me$)(NO)(PPh_3)]BF_4 (14a). Reaction of [Ru(bdmpza)($O_2CC(O)Me$)(PPh_3)] (**3a**) (480 mg, 0.688 mmol) with [NO]BF_4 (166 mg, 1.42 mmol) in CH_2Cl_2 (30 mL) for 1 h at 40 °C afforded according to method D the product [Ru(bdmpza)(O_2CC-(O)Me)(NO)(PPh_3)]BF_4 (**14a**) as a pale red powder.

Yield 468 mg (0.575 mmol, 84%). mp 125 °C (dec.). IR (CH_2Cl_2): $\tilde{\nu}$ = 1912 vs (NO), 1706 s (CO_2^-), 1653 m (CO_2^-), 1560 m (C=N), 1483 w, 1465 w, 1437 m, 1419 vw cm^{-1}. IR (KBr): $\tilde{\nu}$ = 1904 vs (NO), 1692 vs (CO_2^-), 1650 m (CO_2^-), 1562 m (C=N), 1484 w, 1467 w, 1462 w, 1439 m, 1421 vw, 1416 vw cm^{-1}. UV/vis (CH_2Cl_2): λ_{max}/nm (log ε) = 237.0 (4.36), 276.0 (4.29). FAB MS (NBOH): *m*/*z* (%) = 729 (100) [M^+ + H], 641 (52) [$M^+ - O_2CC(O)Me$], 363 (21) [M^+ − bdmpza − $O_2CC(O)Me$ − NO]. ^1H NMR ($CDCl_3$, 250 MHz): δ = 2.01 (s, 3H, C^3-CH_3), 2.24 (s, 3H, $C^{3'}$-CH_3), 2.31 (s, 3H, C(O)-CH_3), 2.57 (s, 3H, $C^{5'}$-CH_3), 2.64 (s, 3H, C^5-CH_3), 6.26 (s, 1H, $H_{pz'}$), 6.32 (s, 1H, H_{pz}), 6.73 (s, 1H, CH), 7.38 (m, 6H, *o*-PPh_3), 7.49 (m, 6H, *m*-PPh_3), 7.64 (m, 3H, *p*-PPh_3). ^{13}C NMR ($CDCl_3$, 100 MHz): δ = 11.1 ($C^{5'}$-CH_3), 11.5 (C^5-CH_3), 13.5 ($C^{3'}$-CH_3), 14.2 (C^3-CH_3), 27.6 (C(O)-CH_3), 68.1 (CH), 110.3 (d, $C^{4'}$, $^4J_{CP}$ = 3.0 Hz), 111.6 (C^4), 124.8 (d, *i*-PPh_3, $^1J_{CP}$ = 54.5 Hz), 129.7 (d, *m*-PPh_3, $^3J_{CP}$ = 11.4 Hz), 133.2 (*p*-PPh_3), 133.5 (d, *o*-PPh_3, $^2J_{CP}$ = 9.8 Hz), 145.4 (d, $C^{5'}$, $^5J_{CP}$ = 1.7 Hz), 147.0 (C^5), 154.2 (d, $C^{3'}$, $^3J_{CP}$ = 2.1 Hz), 158.2 (C^3), 163.3 (CO_2^-), 168.3 (C(O)-CO_2^-), 192.9 (C=O). ^{31}P NMR ($CDCl_3$, 161.8 MHz): δ = 24.1. Anal. Calcd for $C_{33}H_{33}BF_4N_5O_6$-PRu (814.50): C, 48.66; H, 4.08; N, 8.60. Found: C, 48.04; H, 4.20; N, 8.77.

[Ru(bdmpza)($O_2CC(O)Et$)(NO)(PPh_3)]BF_4 (14b). Reaction of [Ru(bdmpza)($O_2CC(O)Et$)(PPh_3)] (**3b**) (450 mg, 0.632 mmol) with [NO]BF_4 (151 mg, 1.29 mmol) in CH_2Cl_2 (50 mL) for 1 h at 40 °C according to method D afforded the product [Ru(bdmpza)(O_2-$CC(O)Et$)(NO)(PPh_3)]BF_4 (**14b**) as a pale red powder.

Yield 500 mg (0.603 mmol, 95%). mp 120 °C (dec.). IR (CH_2Cl_2): $\tilde{\nu}$ = 1911 vs (NO), 1670 s (CO_2^-), 1653 m (CO_2^-), 1561 m (C=N), 1483 w, 1462 w, 1437 m, 1419 vw cm^{-1}. IR (KBr): $\tilde{\nu}$ = 1904 vs (NO), 1701 vs (CO_2^-), 1649 s (CO_2^-), 1561 m (C=N), 1484 w, 1462 w, 1438 m, 1421 vw cm^{-1}. UV/vis (CH_2Cl_2): λ_{max}/nm (log ε) = 237.0 (4.37), 276.0 (4.31). FAB MS (NBOH): *m*/*z* (%) = 743 (100) [M^+ + H], 641 (48) [$M^+ - O_2CC(O)Et$], 566 (21) [$M^+ - O_2CC(O)Et - CO_2$ − NO], 363 (22) [M^+ − bdmpza − $O_2CC(O)Et$ − NO]. ^1H NMR ($CDCl_3$, 400 MHz): δ = 1.08 (t, 3H, CH_2−CH_3, $^3J_{HH}$ = 7.2 Hz), 2.01 (s, 3H, C^3-CH_3), 2.25 (s, 3H, $C^{3'}$-CH_3), 2.56 (s, 3H, $C^{5'}$-CH_3), 2.64 (s, 3H, C^5-CH_3), 2.71 (dq, 1H, CH_2, $^2J_{HH}$ = 19.1 Hz, $^3J_{HH}$ = 7.2 Hz), 2.76 (dq, 1H, CH_2, $^2J_{HH}$ = 19.1 Hz, $^3J_{HH}$ = 7.2 Hz), 6.27 (s, 2H, $H_{pz'}$), 6.32 (s, 2H, H_{pz}), 6.72 (s, 1H, CH), 7.37 (m, 6H, *o*- or *m*-PPh_3), 7.49 (m, 6H, *o*- or *m*-PPh_3), 7.63 (m, 3H, *p*-PPh_3). ^{13}C NMR ($CDCl_3$, 100 MHz): δ = 7.00 (CH_2-CH_3), 11.1 ($C^{5'}$-CH_3), 11.5 (C^5-CH_3), 13.6 ($C^{3'}$-CH_3), 14.2 (C^3−CH_3), 33.6 (C(O)-CH_2), 68.1 (CH), 110.2 (d, $C^{4'}$, $^4J_{CP}$ =

Table 1. Structure Determination Details of Compounds **4**, **5a**, **7a**, and **8b**

	4	5a	7a	8b
empirical formula	$C_{32}H_{33}ClN_5O_2PRu \times 2CH_2Cl_2$	$C_{34}H_{36}N_5O_4PRu \times 2CH_2Cl_2$	$C_{37}H_{38}N_5O_4PRu$	$C_{39}H_{40}N_5O_5PRu \times CH_2Cl_2$
formula weight	856.98	880.57	748.76	875.73
space group (No.), Z	$P2_1/a$ (14), 4	$P\bar{1}$ (2), 2	$P2_1/c$ (14), 4	$P\bar{1}$ (2), 2
a [Å]	17.715(4)	9.792(4)	11.046(3)	10.403(14)
b [Å]	10.9196(11)	12.224(5)	17.400(4)	14.176(10)
c [Å]	20.288(4)	16.944(6)	17.876(4)	14.692(19)
α [°]	90	88.22(4)	90	87.39(10)
β [°]	110.040(9)	75.73(7)	98.58(2)	73.93(13)
γ [°]	90	85.50(4)	90	74.72(9)
V [Å^3]	3686.8(11)	1959.3(13)	3397.3(14)	2008(4)
θ [°]	2.14−26.98	1.24−27.49	1.64−24.07	2.04−26.98
μ(Mo Kα) [mm^{-1}]	0.87	0.758	0.557	0.613
D_c [g cm^{-3}]	1.544	1.493	1.464	1.449
T [K]	200(2)	200(2)	233(2)	123(2)
reflections collected	8269	9271	10482	9208
indep. reflections	8001	8965	5374	8732
obs. refl. ($>2\sigma(I)$)	5962	6605	3327	6925
R_1[a], wR_2[b] (obs.)	0.0441, 0.1015	0.0713, 0.1937	0.0361, 0.0694	0.0469, 0.1076
R_1[a], wR_2[b] (overall)	0.0747, 0.1085	0.1032, 0.2088	0.0933, 0.0782	0.0688, 0.1169

[a] $R_1 = \sum||F_o| - |F_c||/\sum|F_o|$. [b] $wR_2 = \{\sum[w(F_o^2 - F_c^2)^2]/\sum[w(F_o^2)^2]\}^{1/2}$.

3.1 Hz), 111.7 (C^4), 124.8 (d, *i*-PPh_3, $^1J_{CP}$ = 55.4 Hz), 129.7 (d, *m*-PPh_3, $^3J_{CP}$ = 11.4 Hz), 133.2 (*p*-PPh_3), 133.5 (d, *o*-PPh_3, $^2J_{CP}$ = 9.8 Hz), 145.3 (d, $C^{5'}$, $^5J_{CP}$ = 2.1 Hz), 147.0 (C^5), 154.2 (d, $C^{3'}$, $^3J_{CP}$ = 2.1 Hz), 158.2 (C^3), 163.4 (CO_2^-), 168.8 (C(O)-CO_2^-), 196.0 (C=O). ^{31}P NMR ($CDCl_3$, 161.8 MHz): δ = 24.0. Anal. Calcd for $C_{34}H_{35}BF_4N_5O_6PRu$ (828.53): C, 49.29; H, 4.26; N, 8.45. Found: C, 49.29; H, 4.20; N, 8.30.

[Ru(bdmpza)(O_2CC(O)Ph)(NO)(PPh_3)]BF_4 (14c). Reaction of [Ru(bdmpza) (O_2CC(O)Ph)(PPh_3)] (**3c**) (554 mg, 0.729 mmol) with [NO]BF_4 (163 mg, 1.40 mmol) in CH_2Cl_2 (40 mL) for 1 h at 40 °C according to method D afforded the product [Ru(bdmpza)(O_2CC-(O)Ph)(NO)(PPh_3)]BF_4 (**14c**) as a pale red powder.

Yield 629 mg (0.718 mmol, 98%). mp 135 °C (dec.). IR (CH_2Cl_2): $\tilde{\nu}$ = 1911 vs (NO), 1697 s (CO_2^-), 1647 m (CO_2^-), 1562 m (C=N), 1483 w, 1462 w, 1450 w, 1437 m, 1418 vw cm^{-1}. IR (KBr): $\tilde{\nu}$ = 1906 vs (NO), 1690 vs (CO_2^-), 1647 m (CO_2^-), 1595 w, 1561 m (C=N), 1483 w, 1463 w, 1450 vw, 1437 m, 1420 vw cm^{-1}. UV/vis (CH_2Cl_2): λ_{max}/nm (log ε) = 238.0 (4.42), 267.0 (4.47). FAB MS (NBOH): *m*/*z* (%) = 791 (100) [M^+ + H], 641 (51) [M^+ − bF], 566 (21) [M^+ − bF − CO_2 − NO], 363 (37) [M^+ − bdmpza − bF − NO]. ^{1}H NMR ($CDCl_3$, 250 MHz): δ = 1.93 (s, 3H, C^3-CH_3), 2.35 (s, 3H, $C^{3'}$-CH_3), 2.55 (s, 3H, $C^{5'}$-CH_3), 2.62 (s, 3H, C^5-CH_3), 6.25 (s, 1H, $H_{pz'}$), 6.26 (s, 1H, H_{pz}), 6.70 (s, 1H, CH), 7.35−7.70 (m, 18H, Ph and PPh_3), 7.97 (d, 2H, *o*-Ph). ^{13}C NMR ($CDCl_3$, 100 MHz): δ = 11.1 ($C^{5'}$-CH_3), 11.4 (C^5-CH_3), 13.9 ($C^{3'}$-CH_3), 14.2 (C^3-CH_3), 68.1 (CH), 110.1 (d, $C^{4'}$, $^4J_{CP}$ = 3.9 Hz), 111.6 (C^4), 124.7 (d, i-PPh_3, $^1J_{CP}$ = 54.6 Hz), 128.9 (*p*-PPh_3), 129.8 (d, *m*-PPh_3, $^3J_{CP}$ = 11.3 Hz), 129.9 (*o*-Ph), 133.0 (*i*-Ph), 133.2 (*m*-Ph), 133.5 (d, *o*-PPh_3, $^2J_{CP}$ = 9.8 Hz), 134.7 (p-Ph), 145.6 ($C^{5'}$), 147.1 (C^5), 154.1 (d, $C^{3'}$, $^3J_{CP}$ = 2.6 Hz), 158.2 (C^3), 163.3 (CO_2^-), 169.3 (BF-CO_2^-), 186.7 (C=O). ^{31}P NMR ($CDCl_3$, 161.8 MHz): δ = 23.8. For further purification red microystals of **14c** were obtained from a CH_2Cl_2 solution layered with a 1:1 mixture (v/v) of pentane/diethylether. According to the ^{1}H NMR spectrum these crystals contained also half an equivalent CH_2Cl_2. Anal. Calcd for $C_{38}H_{35}BF_4N_5O_6PRu \times {}^1/_2CH_2Cl_2$ (919.04): C, 50.32; H, 3.95; N, 7.62. Found: C, 49.96; H, 3.93; N, 7.97.

Calculations. All density-functional theory (DFT)-calculations were carried out by using the Jaguar 6.0012[8] software running on Linux 2.4.18−14smp on five Athlon MP 2800+ dual-processor workstations (Beowulf-cluster) parallelized with MPICH 1.2.4. X-ray structures or MM2 optimized structures were used as starting geometries. Complete geometry optimizations were carried out on the implemented LACVP* (Hay−Wadt effective core potential (ECP) basis on heavy atoms, N31G6* for all other atoms) basis set and with the BP86 density functional. Orbital plots[9] were obtained using Maestro 7.0.113, the graphical interface of Jaguar.

Rotational barriers have been calculated fully relaxed, fixating one torsion angle around the rotated bond, and optimizing all remaining degrees of freedom. Torsion angles were modified in steps of 5° beginning from the structure of minimum energy.

X-ray Structure Determinations. Single crystals of **4**, **5a**, **7a**, **8b**, **9b**, **10b**, and **14a** were placed with Paratone-N or glue onto a glass fiber. A modified Siemens P4-Diffractometer and an Enraf Nonius CAD4-Mach3 diffractometer were used for data collection (graphite monochromator, Mo Kα radiation, λ = 0.71073 Å, scan rate 4−30° min^{-1}). The structures were solved by using either direct or Patterson methods {Siemens SHELXS-93[10]} and refined with full-matrix least-squares against F^1 {Siemens SHELXL-97[10]}. A weighting scheme was applied in the last steps of the refinement with $w = 1/[\sigma^2(F_o^2) + (aP)^2 + bP]$ and $P = [2F_c^2 + \mathrm{Max}(F_o^2,0)]/3$. The hydrogen atoms were included in calculated positions and refined in a "riding model". In the asymmetric units of **8b** and **14a** one molecule of dichloromethane was co-crystallized per complex molecule, and so were two dichloromethane molecules in the complexes **4**, **5a**, and **10b**. In case of complex **9b** two chloroform molecules were found per asymmetric unit. All cocrystallized solvent molecules were included into the models and refined anisotropically. The PPh_3 as well as the 2-oxocarboxylato ligand exhibited a severe disorder in case of **8b**. Thus, several restraints had to be applied, and the structure allows no detailed discussion of distances and angles. The structure pictures were prepared with the program Diamond 2.1e.[11] All details and parameters of the measurements are summarized in Tables 1 and 2.

Results and Discussion

In a first attempt to exchange one PPh_3 for an acetonitrile ligand, the chlorido complex [Ru(bdmpza)Cl(PPh_3)$_2$] (**1**) was

(8) *Jaguar*, version 6.0; Schrödinger, LLC: New York, NY, 2005.
(9) Stowasser, R.; Hoffmann, R. *J. Am. Chem. Soc.* **1999**, *121*, 3414–3420.
(10) Sheldrick, G. M.; *SHELX-97, Programs for Crystal Structure Analysis*; University of Göttingen, Göttingen, Germany, 1997.
(11) (a) Brandenburg, K.; Berndt, M. *Diamond - Visual Crystal Structure Information System*; Crystal Impact GbR: Bonn, Germany, 1999; (b) for Software Review see Pennington, W. T. *J. Appl. Crystallogr.* **1999**, *32*, 1028–1029.

Table 2. Structure Determination Details of Compounds **9b**, **10b**, and **14a**

	9b	**10b**	**14a**
empirical formula	$C_{38}H_{35}N_4O_5PRu \times 2CHCl_3$	$C_{37}H_{35}N_4O_6PRuS \times 2CH_2Cl_2$	$C_{33}H_{33}BF_4N_5O_6PRu \times CH_2Cl_2$
formula weight	998.48	965.64	899.42
space group (No.), Z	$P2_1/c$ (14), 4	$P2_1/n$ (14), 4	$P\bar{1}$ (2), 2
a [Å]	11.809(7)	10.863(6)	9.516(4)
b [Å]	14.330(2)	14.380(8)	11.297(8)
c [Å]	26.428(8)	26.060(13)	18.399(8)
α [°]	90	90	85.67(5)
β [°]	102.08(7)	90.07(5)	86.36(4)
γ [°]	90	90	75.70(5)
V [Å^3]	4373(3)	4074(4)	1909.1(17)
θ [°]	2.10 − 27.01	2.03 − 25.02	2.11 − 27.00
μ(Mo Kα) [mm^{-1}]	0.809	0.789	0.663
D_c [g cm^{-3}]	1.517	1.574	1.565
T [K]	188(2)	188(2)	188(2)
reflections collected	9994	7565	9776
indep. reflections	9532	7160	7677
obs. refl. ($>2\sigma(I)$)	7359	4276	5681
R_1[a], wR_2[b] (obs.)	0.0612, 0.1540	0.0628, 0.1127	0.0497, 0.1035
R_1[a], wR_2[b] (overall)	0.0821, 0.1693	0.1323, 0.1372	0.0819, 0.1197

[a] $R_1 = \sum||F_o| - |F_c||/\sum|F_o|$. [b] $wR_2 = \{\sum[w(F_o^2 - F_c^2)^2]/\sum[w(F_o^2)^2]\}^{1/2}$.

Scheme 1. Syntheses of Acetonitrile Complexes

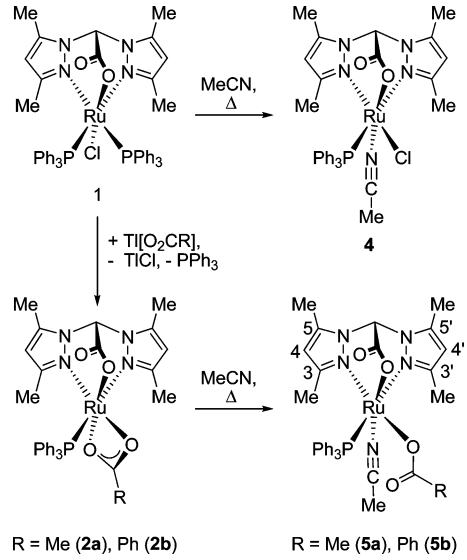

heated under reflux in acetonitrile. Indeed, one PPh_3 ligand is released and the chiral acetonitrile complex [Ru(bdmpza)Cl(NCMe)(PPh_3)] (**4**) is formed when the PPh_3 is extracted with *n*-pentane, although this procedure has to be repeated several times to obtain a complete conversion (Scheme 1).

The complex **4** exhibits two sets of signals for the pyrazolyl donors in the ^{1}H and ^{13}C NMR spectra. The acetonitrile signals have been assigned to 1.88 ppm in the ^{1}H NMR spectrum and to 3.67 and 124.0 ppm in the ^{13}C NMR spectrum. Only one singlet for a single PPh_3 ligand is found in the ^{31}P NMR spectrum at 48.8 ppm. The IR signal of the coordinated acetonitrile is observed at 2275 cm^{-1}. The ^{31}P resonance as well as the IR signal of the coordinated acetonitrile agree well with those reported for the analogous complex [RuTpCl(NCMe)(PPh_3)] (^{31}P: 51.7 ppm; IR: $\tilde{\nu}$(CN) = 2275 cm^{-1}, see Table 3).[6]

As described above, we already observed a hemilabile coordination of the 2-oxocarboxylato ligands. Usually

(12) Gemel, C.; Trimmel, G.; Slugovc, C.; Kremel, S.; Mereiter, K.; Schmid, R.; Kirchner, K. *Organometallics* **1996**, *15*, 3998–4004.

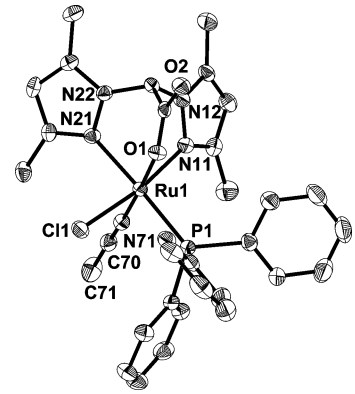

Figure 1. Molecular structure of [Ru(bdmpza)Cl(NCMe)(PPh_3)] (**4**) with thermal ellipsoids drawn at the 50% probability level. Hydrogen atoms and solvent molecules are omitted for clarity.

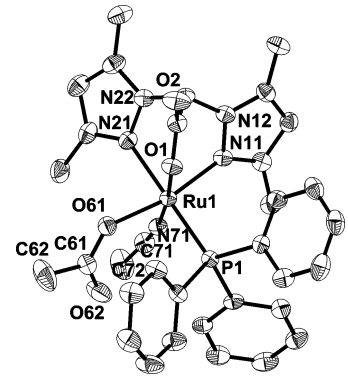

Figure 2. Molecular structure of [Ru(bdmpza)(O_2CMe)(NCMe)(PPh_3)] (**5a**) with thermal ellipsoids drawn at the 50% probability level. Hydrogen atoms and solvent molecules are omitted for clarity.

[Ru(bdmpza)(O_2CC(O)Ph)(PPh_3)] (**3c**) with the κ^2O^1,O^2-coordinated 2-oxocarboxylato ligand exhibits a purple color due to a MLCT transition.[3b] Acetonitrile solutions of **3c** changed to yellow upon standing within some days, clearly indicating a change to κ^1O^1-coordination and the formation of [Ru(bdmpza)(O_2CC(O)Ph)(NCMe)(PPh_3)] (**3c** × NCMe).[3b] Now, we achieved a controlled synthesis of **3c** × NCMe by reacting [Ru(bdmpza)(O_2CC(O)Ph)(PPh_3)] (**3c**) under reflux with acetonitrile for 2 h. An analogous reaction with the 2-oxocarboxylato complexes [Ru(bdmpza)(O_2CC(O)Me)(PPh_3)] (**3a**) and [Ru(bdmpza)(O_2CC(O)Et)(PPh_3)] (**3b**) was not successful so far. On the other hand, we reacted the $\kappa^2O^1,O^{1'}$-carboxylato complexes [Ru(bdmpza)(O_2CMe)(PPh_3)] (**2a**) and [Ru(bdmpza)(O_2CPh)(PPh_3)] (**2b**) with acetonitrile within 5 h to form the carboxylato complexes [Ru(bdmpza)(O_2CCH_3)(NCMe)(PPh_3)] (**5a**) and [Ru(bdmpza)(O_2CPh)(NCMe)(PPh_3)] (**5b**) (Scheme 1).

The acetato complex **5a** exhibits two sets of signals for the diastereotopic pyrazolyl groups in the ^{1}H and ^{13}C NMR spectra. One signal at 2.22 ppm in the ^{1}H NMR spectrum and two signals at 4.60 and 124.7 ppm in the ^{13}C NMR have been assigned to the acetonitrile ligand. The ^{31}P NMR singlet of the PPh_3 ligand was observed at 53.4 ppm. X-ray structure determinations revealed the molecular structures of **4** and **5a** which are depicted in Figures 1 and 2. Selected bond lengths and angles are reported in Table 4. The coordination geometry of these complexes is approximately octahedral, and the distances and angles in these two complexes are

relatively uniform. Because of the space groups $P2_1/a$ and $P\bar{1}$, both enantiomers of the chiral complexes **4** and **5a** can be found in the unit cells. The distances and angles agree well with those of complex **1** which we reported on lately.[3a] It is interesting to note that the positions of the chlorido ligand and also the acetato ligand are *trans* to a pyrazol donor of the bdmpza ligand. In contrast, so far most molecular structures showed a chlorido ligand *trans* to the carboxylato donor of the bdmpza ligand.[3,4]

The complex [Ru(bdmpza)(O_2CPh)(NCMe)(PPh_3)] (**5b**) does form two isomers which show a rather similar pattern in the NMR spectra. The acetonitrile signals have been assigned for both isomers (^{1}H NMR: 2.23 and 1.92 ppm; ^{13}C NMR: 2.23, 124.7, and 3.56, 124.1 ppm). The two signals in the ^{31}P NMR spectrum at 53.6 and 51.9 ppm are due to the PPh_3 ligands of the two isomers. So far, we could not deduce which of the three possible structural isomers are preferentially formed, but we assume one isomer might have a configuration similar to **5a** and the other one a configuration with the benzoato ligand *trans* to the bdmpza carboxylato donor.

The CO_2^- signals in the ^{13}C NMR spectra of the acetato or benzoato ligand in **5a** and **5b**, respectively, have been shifted by 9 ppm to higher field compared to **2a** and **2b**, on account of the κ^1O^1-coordination of the acetato and benzoato ligand. The IR bands assigned to $\tilde{\nu}$(C≡N) of the acetonitrile ligands at 2271 (**5a**) and 2270 cm^{-1} (**5b**) are reasonable compared to other complexes such as those of the Tp complex [RuTpCl(NCMe)(PPh_3)][6] (see Table 3). In the FAB mass spectra molecular mass peaks fit to [Ru(bdmpza)(O_2CMe)(NCMe)(PPh_3)] (**5a**) and [Ru(bdmpza)(O_2CPh)(NCMe)(PPh_3)] (**5b**), although the 100% peaks are assigned to [Ru(bdmpza)(O_2CMe)(PPh_3)] (**2a**) and [Ru(bdmpza)(O_2CPh)(PPh_3)] (**2b**).

Because of the problems that came about in these reactions of the acetonitrile sp-*N* donor with the carboxylato and 2-oxocarboxylato complexes, pyridine has been tested as sp^2-*N* donor ligand instead. A complete conversion within 3 days could be achieved to give complexes **7** and **8**, respectively, for the carboxylato complexes **2a** and **2b** as well as for the 2-oxocarboxylato complexes **3a**−**3c** (Scheme 2) by using 10 equiv of pyridine in dichloromethane.

A similar reaction with [Ru(bdmpza)Cl(PPh_3)$_2$] (**1**) was also successful and afforded the complex [Ru(bdmpza)-Cl(PPh_3)(py)] (**6**). All pyridine complexes **6**, **7a**, **7b**, and **8a**−**8c** exhibit ^{1}H and ^{13}C NMR spectra typical for chiral complexes with two sets of pyrazolyl signals. The PPh_3 singlets in the ^{31}P NMR spectra appear around 50 ppm and are thus shifted by 10 ppm to higher field compared to the educt complexes. Mass peaks in the FAB mass spectra affirm the composition of the complexes.

The ^{13}C NMR CO_2^- signals of the κ^1O^1-coordinated carboxylato ligands are shifted by 11 ppm to higher field compared to the κ^2-carboxylato complexes (178.0 (**7a**) and 171.1 ppm (**7b**)). The ketocarbonyl signals of the 2-oxocarboxylato complexes exhibit a similar 15 ppm shift to higher

Scheme 2. Syntheses of Pyridine Complexes

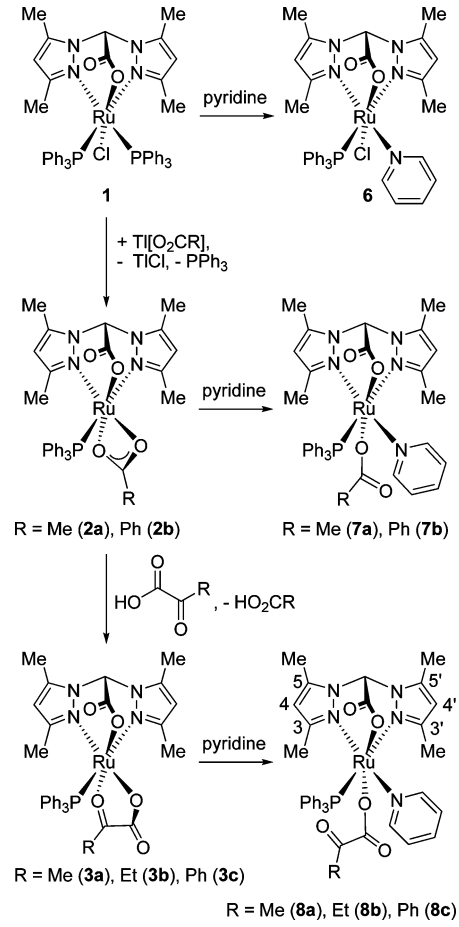

Table 3. Spectroscopic Data of Various Ruthenium Acetonitrile Complexes

complex	IR (C≡N) [cm^{-1}]	^{1}H (MeCN) [ppm]	^{13}C (MeCN) [ppm]	^{31}P [ppm]
[Ru(bdmpza)Cl(NCMe)(PPh_3)] (**4**)	2275[a]	1.88	3.67	48.8
	2269[b]		124	
[Ru(bdmpza)(O_2CMe)(NCMe)(PPh_3)] (**5a**)	2271[a]	2.22	4.6	53.4
	2263[b]		124.7	
[Ru(bdmpza)(O_2CPh)(NCMe)(PPh_3)] (**5b**)	2270[a]	2.23	2.23; 124.7	53.6
	2268[b]	1.92	3.56; 124.1	51.9
[Ru(bdmpza)(O_2CC(O)Ph)(NCMe)(PPh_3)] (**3c** × NCMe)	2278[a]	1.97	3.8	49.7
	2277[b]		n.d.	
[RuTpCl(NCMe)(PPh_3)][6]	2278[b]	2.1		51.7
[RuTpH(NCMe)(PPh_3)][6]	2258[b]	1.69		77.6
[RuTp(dppm)(NCMe)]CF_3SO_3[12]	2284[c]	1.86	4.2	7
			126.2	
[RuTp(NCMe)(pn)]BPh_4[12]	2272[c]	2.34	4.9	69.4
			127.4	

[a] CH_2Cl_2. [b] KBr. [c] Diffuse reflectance.

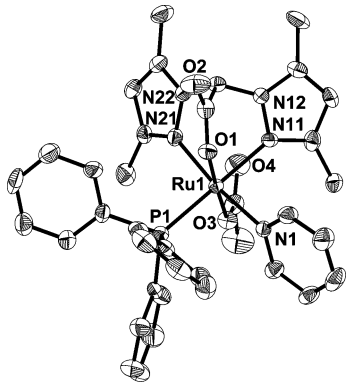

Figure 3. Molecular structure of [Ru(bdmpza)(O_2CMe)(PPh_3)(py)] (**7a**) with thermal ellipsoids drawn at the 50% probability level. Hydrogen atoms and solvent molecules are omitted for clarity.

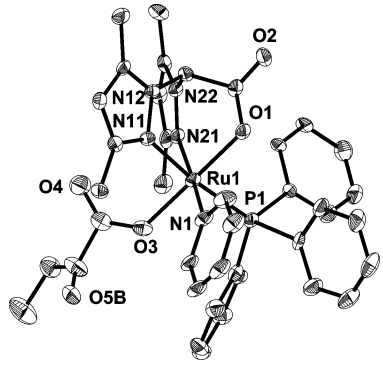

Figure 4. Molecular structure of [Ru(bdmpza)(O_2CC(O)Et)(PPh_3)(py)] (**8b**) with thermal ellipsoids drawn at the 50% probability level. Hydrogen atoms and solvent molecules are omitted for clarity. PPh_3 and $O_2CC(O)CH_2CH_3$ ligands are disordered. Only one of the two alternative orientations that have been included into the structure model is shown here for clarity.

field and are assigned to 197.6 (**8a**), 200.3 (**8b**), and 190.4 ppm (**8c**), respectively. These are typical values of noncoordinated keto ligands.[3b]

Crystals suitable for a single crystal X-ray structure determination have been obtained of [Ru(bdmpza)(O_2CMe)(PPh_3)(py)] (**7a**) and [Ru(bdmpza)(O_2CC(O)Et)(PPh_3)(py)] (**8b**) (Figure 3 and 4; Table 5). The pyridine and the PPh_3 coordinate *trans* to the pyrazolyl groups. The acetato and the 2-oxocarboxylato ligands are *trans* to the carboxylato donor of the bdmpza ligand. Because of a disorder of the PPh_3 and the 2-oxocarboxylato ligands in the molecular structure of **8b**, we will focus on the molecular structure of **7a** for discussion, although both structures are very similar. The distances and angles of the [Ru(bdmpza)(PPh_3)] fragment are almost identical to those of molecular structures of **1**, **2a** × H_2O, and **3b**.[3] The bond lengths of the κ^1-acetato ligand agree well with those of complex **2a** × H_2O, which we reported on recently (**7a**: Ru−O(3) 2.090(3), C(3)−O(3) 1.286(5), C(3)−O(4) 1.221(5); **2a** × H_2O: Ru−O(3) 2.087(3), C(3)−O(3) 1.255(6), C(3)−O(4) 1.220(7)).[3b]

The distance Ru-py in complex [Ru(bdmpza)(O_2CMe)(PPh_3)(py)] (**7a**) is with 2.080(3) Å identical to that in [RuTpCl(PPh_3)(py)] (2.080(7) Å)[13] and agrees also well with those of cationic Tp and Tpm such as [TpRu(OH_2)(py)(=C=C(H)Ph)]OTf (Ru-py = 2.077(3) Å)[14] or [TpmRu(py)$_3$](PF_6)$_2$ (Ru-py = 2.068(5), 2.090(6), and 2.093(6))Å.[15]

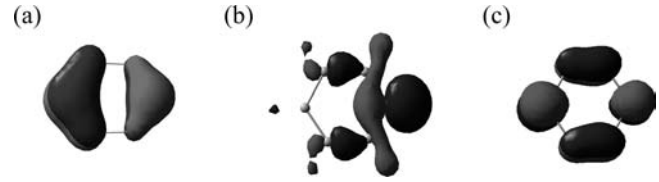

Figure 5. Contour plots (Kohn−Sham orbitals) of (a) the HOMO-2 of pyridine, (b) the HOMO of pyridine, and (c) the LUMO of pyridine.

Although the π-acceptor properties of pyridine are generally accepted to be moderate,[16] the aromatic system of this ligand allows back-bonding as pointed out by the contour plots of its highest occupied molecular orbital (HOMO) and lowest unoccupied molecular orbital (LUMO, Figure 5b and 5c). For a discussion of the almost identical orientation of the pyridine ligands in **7a** and **8b** DFT calculations were performed with the 16 valence electron fragment [Ru(bdmpza)(O_2CPh)(PPh_3)]. Figure 6 shows contour plots of its LUMO, HOMO, HOMO-1, and HOMO-2.

According to these plots, especially the HOMO-2 of the 16 valence electron fragment seems to determine the orientation of the pyridine ligands in the complexes [Ru(bdmpza)(O_2CMe)(PPh_3)(py)] (**7a**) and [Ru(bdmpza)(O_2CC(O)Et)(PPh_3)(py)] (**8b**). The pyridine ligands in **7a** and **8b** are almost in a plane with O(1)−Ru−OAc-N_{py} or O(1)−Ru−$O_{2\text{-oxocarb}}$-N_{py} respectively (Figure 7a and 7b). This orientation allows a $Ru_{d\pi} \rightarrow N_{p\pi}$ back-donation by interaction of the pyridine π^* orbital with the HOMO-2.

Nevertheless, the pyridine ligands in **7a** and **8b** are slightly tilted out of the $O_{carboxylate}$−Ru−N_{py} planes as indicated by the absolute values of the torsion angles [**7a**, $|\angle(O_{OAc}-Ru-N_{py}-C_{py})| = 22.2(2)°$; **8b**, $|\angle(O_{2\text{-oxocarb}}-Ru-N_{py}-C_{py})| = 17.9(3)°$] (Figure 7). This agrees well with the calculated (DFT) structure of minimum energy ($|\angle(O_{OAc}-Ru-N_{py}-C_{py})| = 17.7°$) for complex **7a**. To investigate this deviation from the ideal perpendicular orientation by some 20°, the rotational barrier of the pyridine ligand in [Ru(bdmpza)(O_2CMe)(PPh_3)(py)] (**7a**) has been calculated in steps of 5° beginning from the minimum energy structure (Figure 8). A rotation of the pyridine ligand by 20° causes a rather small increase in energy by 3 to 5 kJ/mol. Thus, this deviation might be due to crystal-packing effects or interactions of the pyridine with PPh_3 or the pyrazolyl Me[3′]. Rather similar findings have been reported recently by us for a vinylidene ligand instead of pyridine in an analogous complex [Ru(bdmpza)Cl(=C=CHTol)(PPh_3)].[4]

Another text book example for a good σ-donor/π-acceptor ligand is the carbonyl ligand. In previous studies with

(13) Pavlik, S.; Puchberger, M.; Mereiter, K.; Kirchner, K. *Eur. J. Inorg. Chem.* **2006**, 4137–4142.

(14) Takahashi, Y.; Akita, M.; Hikichi, S.; Moro-oka, Y. *Inorg. Chem.* **1998**, *37*, 3186–3194.

(15) Laurent, F.; Plantalech, E.; Donnadieu, B.; Jiménez, A.; Hernández, F.; Martínez-Ripoll, M.; Biner, M.; Llobet, A. *Polyhedron* **1999**, *18*, 3321–3331.

(16) (a) Kraihanzel, C. S.; Cotton, F. A. *Inorg. Chem.* **1963**, *2*, 533–540. (b) Graham, W. A. G. *Inorg. Chem.* **1968**, *7*, 315–321. (c) Fielder, S. S.; Osborne, M. C.; Lever, A. B. P.; Pietro, W. J. *J. Am. Chem. Soc.* **1995**, *117*, 6990–6993. (d) Estrin, D. A.; Hamra, O. Y.; Paglieri, L.; Slep, L. D.; Olabe, J. A. *Inorg. Chem.* **1996**, *35*, 6832–6837.

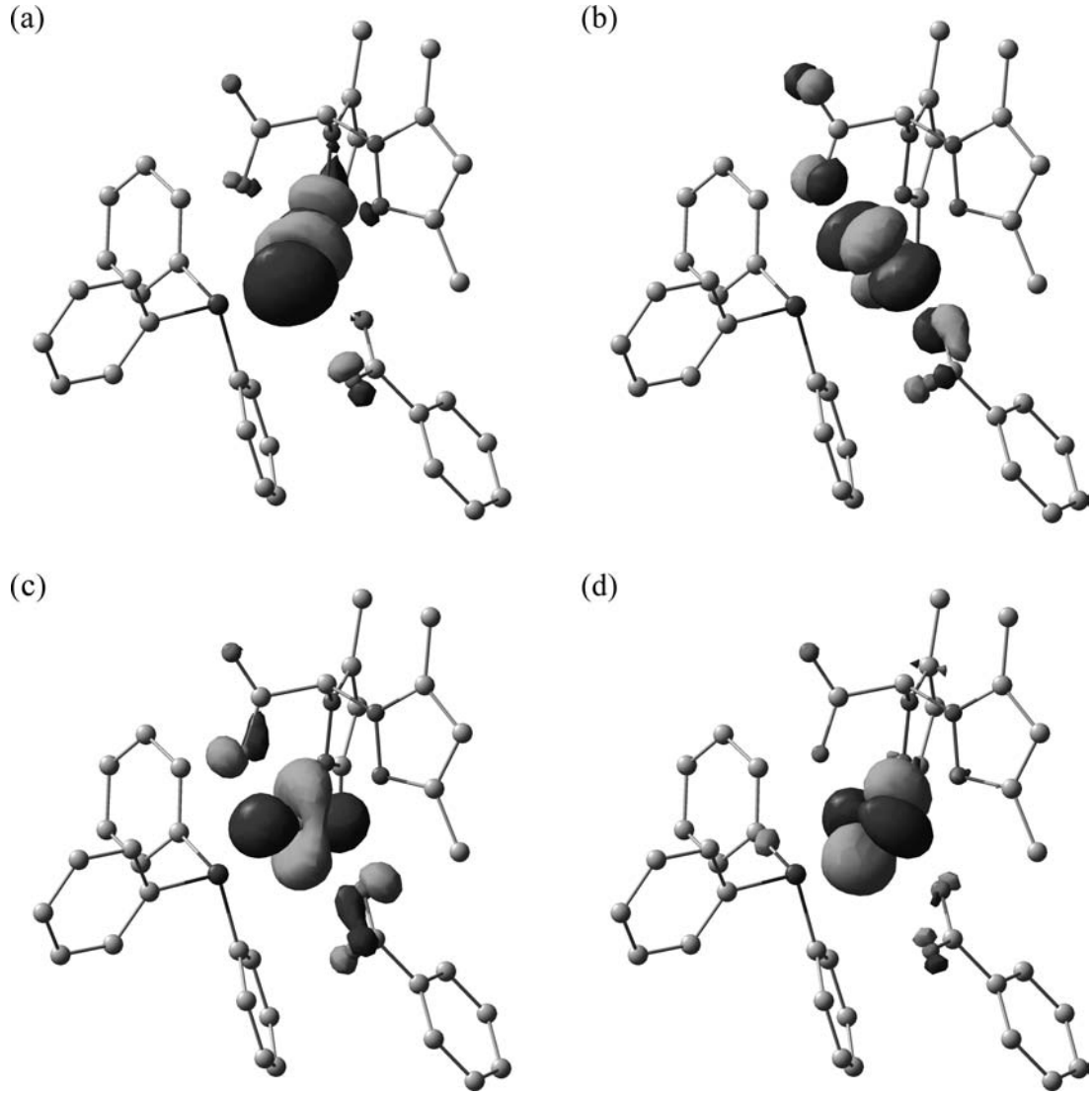

Figure 6. Contour plots (frontier Kohn−Sham orbitals) of the [Ru(bdmpza)(κ^1-O_2CPh)(PPh_3)] 16VE fragment (DFT-calculations) with (a) LUMO, (b) HOMO, (c) HOMO-1, and (d) HOMO-2.

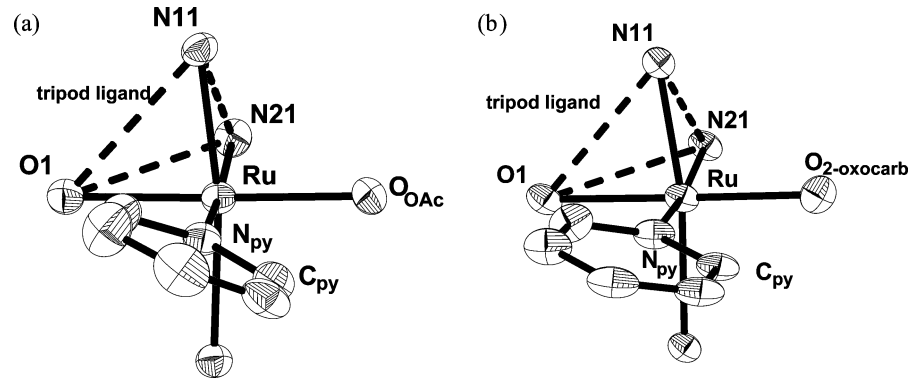

Figure 7. Orientation of the pyridine ligand in (a) [Ru(bdmpza)(O_2CMe)(PPh_3)(py)] (**7a**) and (b) in [Ru(bdmpza)(O_2CC(O)Et)(PPh_3)(py)] (**8b**).

ruthenium vinylidene complexes [Ru(bdmpza)Cl(=C=CHR)-(PPh_3)], as mentioned above, we already obtained a carbonyl complex [Ru(bdmpza)Cl(CO)(PPh_3)] by a degradation reaction.[4] [Ru(bdmpza)Cl(CO)(PPh_3)] can also be obtained by replacing a PPh_3 ligand of [Ru(bdmpza)Cl(PPh_3)$_2$] (**1**) with CO.[4] Therefore, we decided to expose the carboxylato complexes [Ru(bdmpza)(O_2CMe)(PPh_3)] (**2a**) and [Ru-(bdmpza)(O_2CPh)(PPh_3)] (**2b**) to CO. Flushing solutions of **2a** and **2b** with CO gas resulted within 2 h in a complete conversion of these complexes to the carbonyl complexes [Ru(bdmpza)(O_2CMe)(CO)(PPh_3)] (**9a**) and [Ru(bdmpza)-(O_2CPh)(CO)(PPh_3)] (**9b**) (Scheme 3).

Mass spectroscopic data with [M^+] peaks at *m*/*z* 698 (**9a**) and 760 (**9b**) revealed the formation of the carbonyl

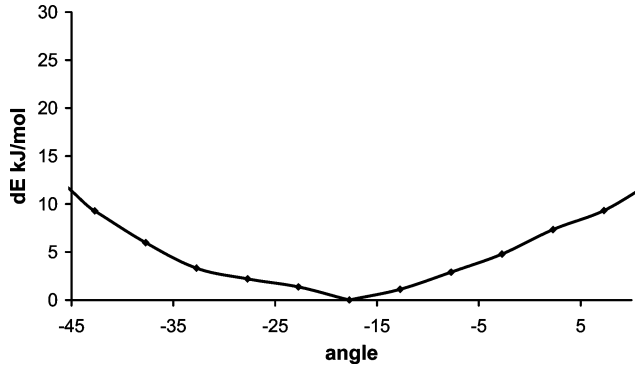

Figure 8. Rotational barrier of the pyridine ligand in [Ru(bdmpza)-(O_2CMe)(PPh_3)(py)] (**7a**), calculated in 5° steps beginning from the structure of minimum energy.

complexes. Because of the chiral C_1 geometry of the complexes, again two sets of signals are observed in the ^{1}H and ^{13}C NMR spectra for the diastereotopic pyrazolyl groups. The ^{13}C NMR carboxylate signals of the κ^1O-coordinated acetato and benzoato ligands are shifted by 11 ppm to higher field (177.3 ppm (**9a**), 172.6 ppm (**9b**)) compared to the complexes **2a** and **2b** with κ^2O,O'-coordination. IR bands at 1669 cm^{-1} (**9a**) and 1669 cm^{-1} (**9b**) are assigned to the asymmetric carboxylate vibrations $\tilde{\nu}_{asym}(CO_2^-)$ of the bdmpza ligand. Two additional bands at 1624 cm^{-1} (**9a**) and 1636 cm^{-1} (**9b**) belong to the carboxylate vibrations $\tilde{\nu}_{asym}(CO_2^-)$ of the κ^1O-coordinated acetato and benzoato ligands. The ^{31}P NMR singlets of the PPh_3 ligands at 43.3 (**9a**) and 43.6 ppm (**9b**) are almost identical to the singlet we reported recently for [Ru(bdmpza)Cl(CO)(PPh_3)] (41.7 ppm).[4] IR signals at 1977 (**9a**) and 1978 (**9b**) cm^{-1} (CH_2Cl_2) and doublets in the ^{13}C{^{1}H} NMR spectra at 205.3 ppm ($^2J_{CP}$ = 19.8 Hz) and 204.2 ppm ($^2J_{CP}$ = 21.2 Hz) can be assigned to the carbonyl ligands and agree also well with the data observed for [Ru(bdmpza)Cl(CO)(PPh_3)].[4] Several carbonyl ruthenium complexes bearing Tp ($BH(pz)_3$), Cp (η^5-C_5H_5), and Cp* (η^5-C_5Me_5) ligands are described in the literature (see Table 6).[17–23]

This allows a closer discussion of the electron donating properties of the bdmpza ligand. The carbonyl vibrations are observed at higher wavenumbers compared to analogous Cp*, Cp, and Tp ruthenium complexes such as [RuCpCl(CO)(PPh_3)] (1958 cm^{-1}), [RuCp*(O_2CMe)(CO)(PPh_3)] (1925 cm^{-1}), or [RuTpCl(CO)(PPh_3)] (1965 cm^{-1}) (Table 4). This implies a weaker $Ru_{d\pi} \rightarrow C_{p\pi}$ back-donation into the carbonyl ligand of the bdmpza complexes. Thus, in these ruthenium complexes the bdmpza ligand seems to be less electron donating compared to Cp*, Cp, and even Tp ligands. Crystals of [Ru(bdmpza)(O_2CPh)(CO)(PPh_3)] (**9b**) suitable for an X-ray structure determination have been obtained from a $CHCl_3$ solution. The molecular structure (Figure 9, Table 7) reveals the formation of a carbonyl complex and the κO^1-coordination of the benzoate ligand *trans* to the bdmpza carboxylate donor.

The Ru−C(3) and C(3)−O(3) bond distances of the carbonyl ligand in **9b** at 1.870(5) Å and 1.145(6) Å are in the expected range of other ruthenium carbonyl complexes (see Table 6).[17–20] These Cp and Tp ruthenium carbonyl complexes show molecular structures with d(Ru−CO) = 1.872(6), d(C−O) = 1.132(8) Å for [RuCpCl(CO)(PPh_3)] and d(Ru−CO) = 1.848(6), d(C−O) = 1.137(8) Å for [RuTpCl(CO)(PPh_3)] (see Table 6). Also, the bond distances of the previously reported complex [Ru(bdmpza)Cl(CO)(PPh_3)] (d(Ru−CO) = 1.821(5) Å, d(C−O) = 1.151(6)) are in this range.[4] The angle Ru−C(3)−O(3) is almost linear (177.0(4)°). The distance d(Ru−N11) = 2.183(3) Å is significantly longer compared to d(Ru−N21) = 2.148(4) Å, indicating the *trans* influence of the carbonyl ligand.

Whereas CO is able to replace one *O*-donor of an hemilabile chelating $\kappa^2O^1,O^{1'}$-carboxylato ligand, an analogous reaction with $\kappa^2O^1,O^{2'}$-oxocarboxylato complexes has not been successful so far. Solutions of [Ru(bdmpza)(O_2CC(O)Me)(PPh_3)] (**3a**) and [Ru(bdmpza)(O_2CC(O)Ph)(PPh_3)] (**3c**) flushed with CO showed only traces of newly formed products beside the educts in the NMR spectra. Thus, 2-oxocarboxylato ligands seem to be tighter bound ligands compared to the carboxylato ligands.

Besides CO, gaseous SO_2 can act as a good σ-donor and π-acceptor ligand too. Various coordination modes to metals are known for SO_2 ligands. A η^1-coordination via the sulfur atom is possible with a planar or a pyramidal geometry. Also a η^2-coordination of SO_2 via a sulfur and an oxygen atom can take place (see Figure 10).[24–27]

Furthermore, SO_2 can be coordinated via the oxygen atom and might also act as a bridging ligand.[25–27] Only a few mainly cationic ruthenium SO_2 complexes such as [RuCp(chir)(SO_2)]PF_6 and [RuCp*(PPh_3)$_2$(SO_2)]Cl have so far been described in the literature.[7b,28–30] Thus, we also investigated the reactivity of carboxylato and 2-oxocarboxylato complexes toward SO_2. Solutions of [Ru(bdmpza)(O_2CMe)(PPh_3)] (**2a**) and [Ru(bdmpza)(O_2CPh)(PPh_3)] (**2c**) in CH_2Cl_2 were flushed with gaseous SO_2 for 30 min to obtain the SO_2 complexes [Ru(bdmpza)(O_2CMe)(PPh_3)(SO_2)] (**10a**) and [Ru(bdmpza)(O_2CPh)(PPh_3)(SO_2)] (**10b**) in high yields (Scheme 3). The IR spectra exhibit two new bands at 1284 and 1128 cm^{-1} (for **10a**) and 1286 and 1129 cm^{-1} (for **10b**). These have been assigned to the

(17) Sun, N.-Y.; Simpson, S. J. *J. Organomet. Chem.* **1992**, *434*, 341–349.
(18) Slugovc, C.; Sapunov, V. N.; Wiede, P.; Mereiter, K.; Schmid, R.; Kirchner, K. *J. Chem. Soc., Dalton Trans.* **1997**, 4209–4216.
(19) Wilczewski, T.; Dauter, Z. *J. Organomet. Chem.* **1986**, *312*, 349–356.
(20) Cao, M.; Do, L. V.; Hoffman, N. W.; Kwan, M.-L.; Little, J. K.; McGilvray, J. M.; Morris, C. B.; Söderberg, B. C.; Wierzbicki, A.; Cundari, T. R.; Lake, C. H.; Valente, E. J. *Organometallics* **2001**, *20*, 2270–2279.
(21) Daniel, T.; Mahr, N.; Braun, T.; Werner, H. *Organometallics* **1993**, *12*, 1475–1477.
(22) Conroy-Lewis, F. M.; Simpson, S. J. *J. Organomet. Chem.* **1987**, *322*, 221–228.
(23) Werner, H.; Braun, T.; Daniel, T.; Gevert, O.; Schulz, M. *J. Organomet. Chem.* **1997**, *541*, 127–147.
(24) Ryan, R. R.; Kubas, G. J.; Moody, D. C.; Eller, P. G. *Struct. Bonding (Berlin)* **1981**, *46*, 47–100.
(25) Kubas, G. J. *Inorg. Chem.* **1979**, *18*, 182–188.
(26) Schenk, W. A. *Angew. Chem., Int. Ed. Engl.* **1987**, *26*, 98–109.
(27) Kubas, G. J. *Acc. Chem. Res.* **1994**, *27*, 183–190.
(28) Schenk, W. A.; Karl, U.; Horn, M. R. *Z. Naturforsch.* **1989**, *44b*, 1513–1518.
(29) Schenk, W. A.; Karl, U. *Z. Naturforsch.* **1989**, *44b*, 988–989.
(30) Schenk, W. A.; Dombrowski, E.; Reuther, I.; Stur, T. *Z. Naturforsch.* **1992**, *47b*, 732–740.

Scheme 3. Syntheses of Carbonyl and SO_2 Complexes

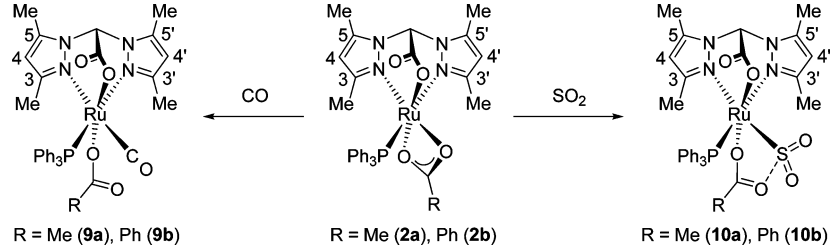

Table 4. Selected Bond Lengths [Å] and Angles [deg] of Complexes **4** and **5a**

	4	5a		4	5a
Ru−N(11)	2.106(3)	2.069(5)	Ru−P	2.3011(10)	2.2969(16)
Ru−N(21)	2.135(3)	2.111(5)	Ru−N(71)	1.993(3)	1.993(5)
Ru−O(1)	2.098(2)	2.099(4)	N(71)−C(71)	1.138(4)	1.135(7)
Ru−Cl	2.4282(9)		C(71)−C(72)	1.454(5)	1.455(8)
Ru−O(61)		2.075(4)			
N(11)−Ru−N(21)	83.20(11)	83.30(18)	O(1)−Ru−N(71)	177.88(11)	174.48(17)
O(1)−Ru−N(11)	86.27(10)	89.04(16)	P(1)−Ru−Cl	86.60(3)	
O(1)−Ru−N(21)	87.12(10)	85.38(17)	P(1)−Ru−O(61)		90.71(13)
O(1)−Ru−P	90.30(7)	88.68(13)	N(11)−Ru−Cl	171.55(8)	
N(21)−Ru−P	174.60(8)	173.79(12)	N(11)−Ru−(O61)		168.03(16)
P−Ru−N(71)	91.69(9)	95.60(15)	Ru−N(71)−C(71)	174.7(3)	168.2(5)

Table 5. Selected Bond Lengths [Å] and Angles [deg] of the Complexes **7a** and **8b**

	7a	8b		7a	8b
Ru−N(11)	2.138(3)	2.115(3)	N(11)−Ru−N(21)	85.71(13)	85.71(15)
Ru−N(21)	2.096(3)	2.089(4)	O(1)−Ru−N(11)	85.27(11)	85.03(13)
Ru−O(1)	2.110(3)	2.108(3)	O(1)−Ru−N(21)	87.39(11)	87.41(16)
Ru−N(1)	2.080(3)	2.095(4)	O(1)−Ru−O(3)	177.31(11)	178.27(9)
Ru−O(3)	2.090(3)	2.097(3)	N(11)−Ru−P	171.02(9)	171.38(8)
Ru−P	2.3051(12)	2.303(3)	N(21)−Ru−N(1)	172.83(13)	173.03(11)
C−O(3)	1.286(5)	1.278(5)			
C−O(4)	1.221(5)	1.223(5)			

asymmetric and symmetric SO_2 vibrations. Such values are typical for SO_2 complexes with a η^1-planar geometry, which usually reveal two bands in between 1300 to 1225 cm^{-1} and 1140 to 1060 cm^{-1}.[24,25] These vibrations of the bdmpza ruthenium SO_2 complexes are found at smaller wavenumbers compared to the cyclopentadienyl complex $[Ru(Cp)(PPh_3)_2(SO_2)]Cl$ (1294 and 1118 cm^{-1})[28] but at higher wavenumbers compared to the Cp* ruthenium complex $[RuCp^*(PPh_3)_2(SO_2)]Cl$ (1277 and 1110 cm^{-1})[28] (see Table 8). The coordination of the SO_2 ligand is also backed by an M^+ peak in the FAB mass spectrum.

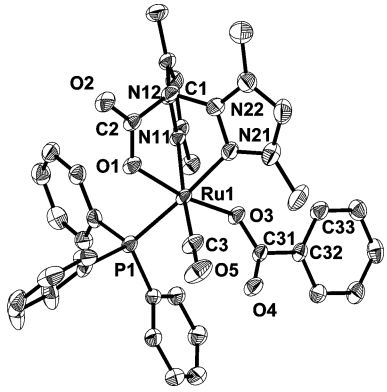

Figure 9. Molecular structure of $[Ru(bdmpza)(O_2CPh)(CO)(PPh_3)]$ (**9b**) with thermal ellipsoids drawn at the 50% probability level. Hydrogen atoms and solvent molecules are omitted for clarity.

The unsymmetrical C_1 geometry of both SO_2 complexes **10a** and **10b** is clearly indicated by two sets of signals in the ^1H and ^{13}C NMR spectra, which have been assigned to the two pyrazolyl donors. The ^{13}C NMR signal of the κ^1O-coordinated carboxylato donor is shifted by 9 ppm to higher field compared to the $\kappa^2O^1,O^{1\prime}$-coordinated carboxylato complexes **2a** and **2b**. This shift and the ^{31}P NMR signals of the PPh_3 ligand at 45.4 and 44.6 ppm agree well with the carbonyl complex data discussed above. Similar to the CO ligand, SO_2 is able to replace one *O*-donor of the hemilabile, chelating $\kappa^2O^1,O^{1\prime}$-carboxylato ligand. Again, a similar reaction of SO_2 with the 2-oxocarboxylato complexes $[Ru(bdmpza)(O_2CC(O)CH_3)(PPh_3)]$ (**3a**), $[Ru(bdmpza)(O_2CC(O)CH_2CH_3)(PPh_3)]$ (**3b**), and $[Ru(bdmpza)(O_2CC(O)Ph)(PPh_3)]$ (**3c**) has not been successful so far. An X-ray structure determination of $[Ru(bdmpza)(O_2CPh)(PPh_3)(SO_2)]$ (**10b**) shows a molecular structure with the SO_2-ligand *trans* to a pyrazolyl donor of the bdmpza ligand (Figure 11, Table 9). This position is also preferred by the other acceptor ligands, such as CO and pyridine (Figures 3, 4, and 10). The bond distances from the bdmpza and PPh_3 ligands to the ruthenium and also the angles between the coordinated

(31) Kovalevsky, A. Y.; Bagley, K. A.; Cole, J. M.; Coppens, P. *Inorg. Chem.* **2003**, *42*, 140–147.

Table 6. Spectroscopic and Structure Data of Various Ruthenium Carbonyl Complexes

complex	IR (CO) [cm^{-1}]	d(Ru−CO)/ d(C−O) [Å]	∠(Ru−C−O) [deg]	^{31}P [ppm]
[Ru(bdmpza)(O_2CMe)(CO)(PPh_3)] (**9a**)	1977[a] 1967[b]			43.3
[Ru(bdmpza)(O_2CPh)(CO)(PPh_3)] (**9b**)	1978[a] 1953[b]	1.870(5) 1.146(6)	177.0(4)	43.6
[Ru(bdmpza)Cl(CO)(PPh_3)][4]	1969[a]	1.821(5) 1.151(6)	178.0(4)	41.7
[RuTpCl(CO)(PPh_3)][17,18]	1965[c]	1.848(6) 1.137(8)	173.2(5)	42.4
[RuCpCl(CO)(PPh_3)][19]	1958[c]	1.911(20) 1.034(27)	176.9(1.2)	
[RuCpCl(CO)(PPh_3)][20]	1959[a]	1.872(6) 1.132(8)	178.3(8)	48.9
[RuCp(O_2CMe)(CO)(PPh_3)][21]	1945[b]			54.3
[RuCp*Cl(CO)(PPh_3)][22]	1918[c]			48.2
[RuCp*(O_2CMe)(CO)(PPh_3)][23]	1925[b]			53.9

[a] CH_2Cl_2. [b] KBr. [c] Nujol.

Table 7. Selected Bond Lengths [Å], Angles [deg], and Torsion Angles [deg] of Complex **9b**

Ru−N(11)	2.183(3)	C(3)−O(5)	1.145(6)
Ru−N(21)	2.148(4)	C(1)−C(2)	1.552(6)
Ru−O(1)	2.115(3)	C(2)−O(1)	1.273(5)
Ru−P	2.3293(17)	C(2)−O(2)	1.233(5)
Ru−O(3)	2.059(3)	C(31)−O(3)	1.297(5)
Ru−C(3)	1.870(5)	C(31)−O(4)	1.231(5)
N(11)−Ru−N(21)	81.41(14)	O(1)−Ru−O(3)	169.37(12)
O(1)−Ru−N(11)	85.89(12)	N(21)−Ru−P	175.49(10)
O(1)−Ru−N(21)	85.54(14)	N(11)−Ru−C(3)	174.56(18)
Ru−C(3)−O(5)	177.0(4)		
O(3)−C(31)−C(32)−C(33)	26.4(6)		

ligands are more or less the same compared to the molecular structures of **2a** × H_2O and **3c**.

The κ^1-benzoato bond lengths of **10b** [d(C(3)−O(5)) = 1.271(8) Å; d(C(3)−O(6)) = 1.272(8) Å] are almost equal. Thus, both oxygen donors seem to share the negative charge of the benzoato ligand. The phenyl group of the benzoato ligand in the SO_2-complex **10b** deviates by −21.1(10)° from the RCO_2-plane. A similar twist by 26.4(6)° is observed for the carbonyl complex **9b**. The η^1-bound SO_2 is not planar but distorted with a distance of 0.685(11) Å between ruthenium and the O(3)−S(1)−O(4) plane. The bond distances S(1)−O(3) [1.452(5) Å] and S(1)−O(4) [1.456(5) Å] agree well with those of other ruthenium SO_2 complexes such as [RuCp(chir)SO_2]PF_6 [1.432(6) and 1.458(6) Å] (see Table 8). The Ru−S(1) distance [2.182(2) Å] is significantly longer than those found in other ruthenium SO_2 complexes like [RuCp(chir)SO_2]PF_6 [2.128(2) Å] or *trans*-[Ru(O_2CCF_3)-(NH_3)$_4$(SO_2)](O_2CCF_3) [2.0945(5) Å].[7b,31]

The S(1)−O(6) distance between the SO_2 and the benzoato ligand is surprisingly short [2.022(5) Å]. In fact, it lies in

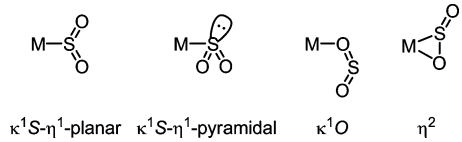

Figure 10. Coordination modes of SO_2 in transition metal complexes.[23–26]

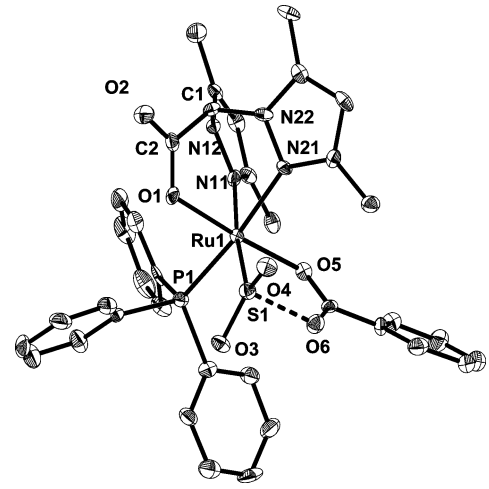

Figure 11. Molecular structure of [Ru(bdmpza)(O_2CPh)(PPh_3)(SO_2)] (**10b**) with thermal ellipsoids drawn at the 50% probability level. Hydrogen atoms and solvent molecules are omitted for clarity.

between the sum of the van der Waals radii (3.25 Å)[32] and a single S−O bond (around 1.6 Å) such as the S-OH bond in the complex [Ru(SO_3H)$_2$(bpy)$_2$] (1.586(5) and 1.612(8)Å).[33] This rather short distance indicates an intramolecular Lewis acid−base interaction between the Lewis acid SO_2 and the uncoordinated carboxylate oxygen. Because of the partial charge at this atom, this oxygen donor should be a rather good Lewis base.

In η^1-planar complexes SO_2 usually binds via the sulfur lone electron pair as a σ-donor to the metal. The LUMO of SO_2 which exhibits a π^* antibonding character, allows that this coordinative bond is enforced via π backdonation by filled metal d orbitals (Figure 6, Figure 12 and 13).[26] A η^1-pyramidal coordination of SO_2 ligands is observed for electron rich complex fragments such as Vaskas SO_2 complex [IrCl(CO)(PPh_3)$_2$(SO_2)].[26] In these η^1-pyramidal SO_2 complexes the bonding electron pair is formally provided by the electron-rich transition metal fragment (Figure 12).[26]

(32) Weast, R. C. *CRC Handbook of Chemistry and Physics*; CRC Press, Boca Raton, 1988; p D-111.
(33) Allen, L. R.; Jeter, D. Y.; Cordes, A. W.; Durham, B. *Inorg. Chem.* **1988**, *27*, 3880–3885.

Table 8. Spectroscopic and Structural Data Of Cp, Cp*, and bdmpza SO_2 Complexes

complex	IR (SO_2) [cm^{-1}]	d(Ru−SO_2)/ d(S−O) [Å]	∠(Ru−S−O)/ ∠(O−S−O) [deg]	^{31}P [ppm]
[Ru(bdmpza)(O_2CMe)(PPh_3)(SO_2)] (**10a**)	1284[a] 1128[a] 1282[b] 1128[b]			45.4
[Ru(bdmpza)(O_2CPh)(PPh_3)(SO_2)] (**10b**)	1286[a] 1129[a] 1283[b] 1125[b]	2.182(2) 1.452(5) 1.456(5)	118.1(2) 124.0(2) 114.2(3)	44.6
[RuCp(chir)(SO_2)]PF_6[7b]	1296[c] 1118[c]	2.128(2) 1.432(6) 1.458(6)	120.9(3) 125.1(3) 113.9(4)	69.3 74.2
[RuCp(PPh_3)$_2$(SO_2)]Cl[28]	1294[c] 1118[c]			32.6
[RuCp*(PPh_3)$_2$(SO_2)]Cl[28]	1277[c] 1110[c]			35.3
trans-[Ru(O_2CCF_3)(NH_3)$_4$(SO_2)] (O_2CCF_3)[31]	1275[b] 1122[b]	2.0945(5) 1.444(2) 1.446(2)		

[a] CH_2Cl_2, [b] KBr, [c] Nujol

Table 9. Selected Bond Lengths [Å] and Angles [deg] of Complex **10b**

Ru−N(11)	2.147(6)	S−O(3)	1.452(5)
Ru−N(21)	2.206(6)	S−O(4)	1.456(6)
Ru−O(1)	2.092(4)	S−O(6)	2.022(5)
Ru−P	2.331(2)	C(3)−O(5)	1.271(8)
Ru−S	2.182(2)	C(3)−O(6)	1.272(8)
Ru−O(5)	2.073(4)	Ru-plane (S1−O3−O4)	0.685(11)
N(11)−Ru−N(21)	79.7(2)	Ru−S(1)−O(3)	124.0(2)
O(1)−Ru−N(11)	88.82(19)	Ru−S(1)−O(4)	118.1(2)
O(1)−Ru−N(21)	86.7(2)	O(3)−S(1)−O(4)	114.2(3)
O(1)−Ru−P(1)	89.25(14)	Σ	356.3(7)
P(1)−Ru−S(1)	91.29(7)		
S(1)−Ru−O(1)	93.90(13)	O(5)−C(3)−C(4)−C(9)	−21.1(10)

A transition from η^1-planar to η^1-pyramidal geometry might be caused if either the σ^* orbital of the M-S bond or the LUMO of SO_2 is occupied and both are of similar energy.[26] Obviously, according to the angles around the SO_2 ligand [∠Ru−S(1)−O(3) = 124.0(2)°, ∠Ru−S(1)−O(4) = 118.1(2)°, and ∠O(3)−S(1)−O(4) = 114.2(3)°], the complex [Ru(bdmpza)(O_2CPh)(PPh_3)(SO_2)] (**10b**) is an almost η^1-planar complex in which SO_2 acts as σ-donor and π-acceptor. Because of the Lewis acid−base interaction between the coordinated SO_2 and the carboxylato ligand, indicated by the short S(1)−O(6) distance [2.022(5) Å], the SO_2 LUMO might be partially occupied. This could explain the slight deviation from the η^1-planar geometry, as well as the rather long Ru−S(1) distance. Until now, in the literature two SO_2 complexes with carboxylato ligands have been described: the mononuclear complex [Ru(O_2CCF_3)(NH_3)$_4$(SO_2)](O_2CCF_3), in which SO_2 coordinates *trans* to the carboxylato ligand, and the dinuclear complex [Mo_2(NTo)$_2$(S_2P(OEt)$_2$)$_2$(μ-O_2CMe)(μ-SBz)(μ-SO_2)], with bridging SO_2 and carboxylato ligands.[31,34] Thus, to the best of our knowledge, **10a** and **10b** are the first examples of intramolecular Lewis acid−base adducts regarding SO_2 complexes.

Table 10. Selected Bond Lengths [Å], Angles [deg], and Torsion Angles [deg] of the Complex **14a**

Ru−N(11)	2.117(4)	C(1)−C(2)	1.562(6)
Ru−N(21)	2.130(3)	C(2)−O(1)	1.308(5)
Ru−O(1)	2.065(3)	C(2)−O(2)	1.205(6)
Ru−P	2.4174(15)	C(41)−O(41)	1.295(5)
Ru−O(41)	2.028(3)	C(41)−O(42)	1.215(5)
Ru−N(31)	1.760(4)	C(41)−C(42)	1.585(7)
N(31)−O(31)	1.145(4)	C(42)−O(43)	1.211(6)
		C(42)−C(43)	1.470(8)
N(11)−Ru−N(21)	83.12(14)	N(11)−Ru−P	95.78(11)
O(1)−Ru−N(11)	85.34(14)	N(21)−Ru−P	175.26(11)
O(1)−Ru−N(21)	86.66(14)	N(21)−Ru−N(31)	94.34(16)
O(1)−Ru−P(1)	88.66(9)	N(31)−Ru−O(41)	97.39(16)
N(21)−Ru−O(41)	91.99(14)	O(1)−Ru−N(31)	93.20(16)
N(11)−Ru−N(31)	177.14(15)	O(1)−Ru−O(41)	169.39(11)
N(11)−Ru−O(41)	84.05(14)	Ru−N(31)−O(31)	177.4(4)
		O(41)−C(41)−C(42)−O(43)	−18.5(7)

Inspired by the reactivity of the carboxylato complexes toward CO and also by other ruthenium nitrosyl complexes described in the literature, such as [RuCpCl(NO)(PPh_3)]PF_6,[35] the complex [Ru(bdmpza)(O_2CC(O)Ph)(PPh_3)] (**3c**) was reacted with gaseous nitric oxide (NO). A significant color change from dark purple to blue was observed. Once the solvent and the excess of NO were removed in vacuo, a red product was obtained. The IR spectrum (CH_2Cl_2) shows two signals at 1698 and 1645 cm^{-1} which have been assigned to asymmetric carboxylate vibrations of the bis(3,5-dimethylpyrazol-1-yl)acetato and the benzoylformato (BF) ligand. A vibration at 1911 cm^{-1} indicates a linear nitrosyl ligand.[36] The ^{1}H and ^{13}C NMR spectra of the diamagnetic complex show two sets of methyl signals for the pyrazoles (^{1}H: 1.95, 2.36, 2.57, and 2.62 ppm; ^{13}C: 11.1, 11.5, 13.9, and 14.3 ppm) as to be expected for an asymmetric geometry of the complex. The ^{13}C NMR signal of the benzoylformate keto group is shifted slightly to higher field (202.8 → 186.7 ppm) compared to that of the educt complex **3c**. This finding is rather similar to the pyridine complex **8c** and consequently indicates an uncoordinated keto group. ^{13}C NMR signals at 163.0 and 169.4 ppm were assigned to the κ^1-coordinated

(34) Wang, R.; Mashuta, M. S.; Richardson, J. F.; Noble, M. E. *Inorg. Chem.* **1996**, *35*, 3022–3030.
(35) Conroy-Lewis, F. M.; Redhouse, A. D.; Simpson, S. J. *J. Organomet. Chem.* **1990**, *399*, 307–315.
(36) Mingos, D. M. P.; Sherman, D. J. *Adv. Inorg. Chem.* **1989**, *34*, 293–377.

Table 11. Spectroscopic and Structural Data of Various Cp, Cp*, Tp, and bdmpza Nitrosyl Complexes

complex	IR (NO) [cm^{-1}]	d(Ru−NO>)/d(N−O) [Å]	∠(Ru−N−O) [deg]	^{31}P [ppm]
$[Ru(bdmpza)(O_2CC(O)Ph)(NO)(PPh_3)]^+$ (**12**)	1911[a]			24.2
	1906[b]			
$[Ru(bdmpza)(O_2CMe)(NO)(PPh_3)]BF_4$ (**13a**)	1912[a]			23.5
	1897[b]			
$[Ru(bdmpza)(O_2CPh)(NO)(PPh_3)]BF_4$ (**13b**)	1912[a]			23.3
	1903[b]			
$[Ru(bdmpza)(O_2CC(O)Me)(NO)$	1912[a]	1.760(4)	177.4(4)	24.1
$(PPh_3)]BF_4$ (**14a**)	1904[b]	1.145(4)		
$[Ru(bdmpza)(O_2CC(O)Et)(NO)$	1911[a]			24
$(PPh_3)]BF_4$ (**14b**)	1904[b]			
$[Ru(bdmpza)(O_2CC(O)Ph)(NO)$	1911[a]			23.8
$(PPh_3)]BF_4$ (**14c**)	1906[b]			
$[Ru(bdmpza)(Cl)_2(NO)]$[5]	1868[a]			
	1872[b]			
$[Ru(bdmpza)_2(NO)]Cl$[5]	1862[a]			
	1860[b]			
$[RuTpCl(CH_2C(O)p\text{-}CH_3C_6H_4)(NO)]$[38]		1.742(2)	178.9(3)	
		1.128(3)		
$[RuCpCl(NO)(PPh_3)]PF_6$[35]	1849[c]	1.775(5)	172.2(5)	37.1
		1.132(7)		
$[RuCp^*(NO)(dppe)](PF_6)_2$[34]	1850[b]	1.748(4)	174.1(4)	66.4
		1.141(5)		

[a] CH_2Cl_2. [b] KBr. [c] Nujol.

carboxylato groups of the bdmpza and BF ligands. The ^{31}P NMR singlet signal of the PPh_3 ligand can be observed at 23.8 ppm. The product of the reaction can be precipitated from dichloromethane by adding diethylether. A molecular mass peak (FAB) at 791 agrees well with a complex cation $[Ru(bdmpza)(O_2CC(O)Ph)(NO)(PPh_3)]^+$ and thus with a coordinated nitrosonium (NO^+) ligand. Obviously, reaction of **3c** with a large excess of gaseous NO results in the formation of a complex cation $[Ru(bdmpza)(O_2CC(O)Ph)(NO)(PPh_3)]^+$ (**12**) (Scheme 4).

One explanation> for this NO^+ formation might be the presence of NO_2 in the reaction mixture, which is almost impossible to prevent in such reactions. Because NO of low purity grade has been used in our reaction, the presence of NO_2 traces is very likely here. It is well-known that this might be a source of NO^+ and NO_3^-.[37] Thus, the counteranion might be nitrate NO_3^-, although nitrite NO_2^- cannot be ruled

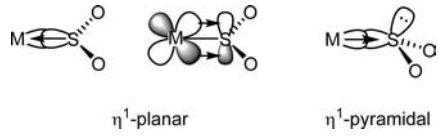

Figure 12. SO_2 as σ-donor/π-acceptor and as σ-acceptor respectively in SO_2 complexes.[23–26]

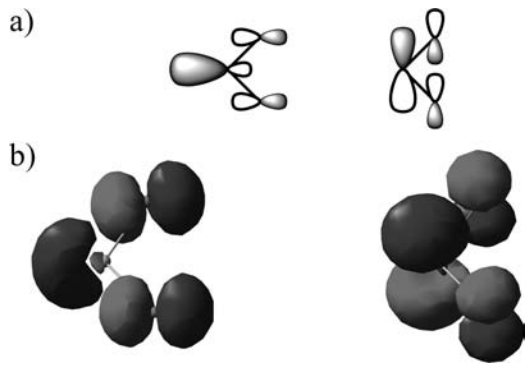

Figure 13. (a) HOMO and LUMO of SO_2 according to literature[23–26] and (b) calculated Kohn-Sham orbitals (DFT).

Scheme 4. Synthesis of Nitrosyl Complexes with Gaseous NO

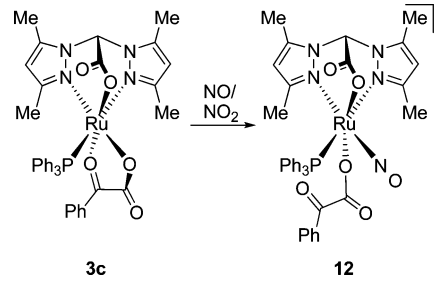

out completely. Indeed analytical test reactions performed with **12** indicated traces of NO_3^- but no NO_2^-. Unfortunately, so far we cannot prove the formation of a NO_3^- counteranion unequivocally.

A similar reaction with an excess of NO is also possible with the acetato complex $[Ru(bdmpza)(O_2CMe)(PPh_3)]$ (**2a**), although no complete conversion could be achieved so far. Nevertheless, we were able to analyze the reaction product $[Ru(bdmpza)(O_2CMe)(NO)(PPh_3)]^+$ (**11**). ^{1}H NMR signals at 1.94, 2.07, 2.25, 2.56, and 2.63 ppm have been assigned to the five methyl groups, and singlets at 6.20, 6.41, and 6.67 ppm belong to the pyrazolyl protons and the CH bridge, thus indicating again an unsymmetrical complex. Similar to the benzoylformato complex **12**, the NO vibration is observed at 1911 cm^{-1} in the IR spectrum. The M^+ peak at 700 in the FAB mass spectrum fits to a $[Ru(bdmpza)(O_2CMe)(NO)(PPh_3)]^+$ cation. Again, the nature of the anion, most likely nitrate NO_3^-, stays unresolved so far.

To verify the nitrosyl complex cations $[Ru(bdmpza)(O_2CMe)(NO)(PPh_3)]^+$ (**11**) and $[Ru(bdmpza)(O_2CC(O)Ph)(NO)$-

(37) Burdinski, D.; Brans, H. J. A.; Decre, M. M. J. *J. Am. Chem. Soc.* **2005**, *127*, 10786–10787.
(38) Arikawa, Y.; Nishimura, Y.; Kawano, H.; Onishi, M. *Organometallics* **2003**, *22*, 3354–3356.
(39) Mauthner, K.; Mereiter, K.; Schmid, R.; Kirchner, K. *Inorg. Chim. Acta* **1995**, *236*, 95–100.
(40) Nagao, H.; Nishimura, H.; Funato, H.; Ichikawa, Y.; Howell, F. S.; Mukaida, M.; Kakihana, H. *Inorg. Chem.* **1989**, *28*, 3955–3959.

Scheme 5. Synthesis of Nitrosyl Complexes with $NO[BF_4]$

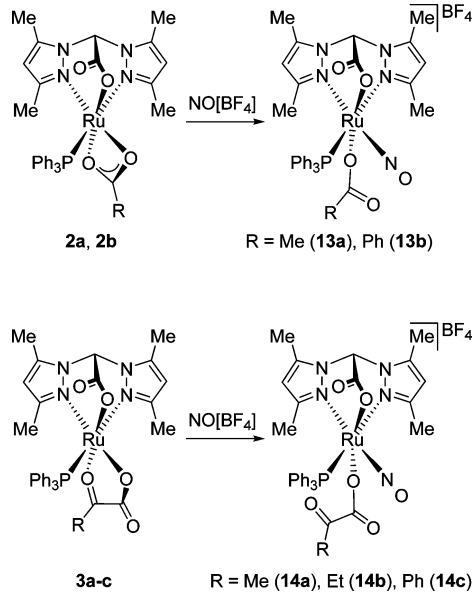

$(PPh_3)]^+$ (**12**), the carboxylato complexes [Ru(bdmpza)-$(O_2CR)(PPh_3)]$ (**3a,b**) (R = Me, Ph), as well as the 2-oxocarboxylato complexes [Ru(bdmpza)$(O_2CC(O)R)$-$(PPh_3)]$ (**3a**−**c**) (R = Me, Et, Ph), were reacted with $[NO]BF_4$ to yield the complexes [Ru(bdmpza)$(O_2CR)(NO)(PPh_3)]BF_4$ (**13a,c**) (R = Me, Ph) and [Ru(bdmpza)$(O_2CC(O)R)$-$(NO)(PPh_3)]BF_4$ (**14a**−**c**) (R = Me, Et, Ph) (Scheme 5.). NMR samples of the complex **11** in combination with **13a** as well as of **12** and **14c** indicated identical cations [Ru(bdmpza)-$(O_2CMe)(NO)(PPh_3)]^+$ and [Ru(bdmpza)$(O_2CC(O)Ph)(NO)$-$(PPh_3)]^+$, respectively, according to the spectroscopic data (^1H, ^{13}C, and ^{31}P). The fact that gaseous NO might be used as NO^+ source has been described before.[39,40] For example Kirchner et al. recently reported on a similar transformation of $[Cp^*Ru(dppe)]PF_6$ to $[Cp^*Ru(dppe)(NO)](PF_6)_2$ by either gaseous NO or $[NO]PF_6$.[39]

In general, the yield of these reactions is rather high (84−98%), and reactions with the carboxylato complexes are faster compared to with the 2-oxocarboxylato complexes. The constitution of the nitrosyl complexes **13a,b** and **14a-c** is backed by M^+ peaks in the FAB mass spectra. The ^{13}C NMR signals assigned to the keto carbons of the nitrosyl 2-oxocarboxylato complexes **14a-c** are shifted to higher field by 15 ppm compared to the educts **3a-c**, thus indicating a κ^1O^1-coordination of the 2-oxocarboxylato ligands. The ^{31}P NMR signals are observed from 23.3 to 24.2 ppm. This means a high field shift of almost 25 ppm compared to the educts. The diamagnetic property observed for the nitrosyl complexes **11**, **12**, **13a**, **13b**, and **14a-c** is typical of the $\{RuNO\}^6$ type of complexes.[41] The NO IR signals [around 1911 cm^{-1} (CH_2Cl_2) and 1897 to 1906 cm^{-1} (KBr)] are lying in between the vibration of free NO^+ (2377 cm^{-1}) and that of NO or NO^- (1860 and 1470 cm^{-1}, respectively),[36,42] indicating a nitrosonium NO^+ ligand. Other cationic ruthenium nitrosyl complexes bearing Cp or Cp* ligands such as $[CpRuCl(PPh_3)(NO)]PF_6$ ($\tilde{\nu}$(NO) = 1849 cm^{-1} (Nujol)) and $[Cp^*Ru(dppe)(NO)](CF_3SO_3)_2$ ($\tilde{\nu}$(NO) = 1850 cm^{-1} (Nujol)) exhibit NO vibrations at lower wavenumbers (see Table 11).[35,39] It is noteworthy that the $\tilde{\nu}$(NO) of bis(3,5-dimethylpyrazol-1-yl)aceto nitrosyl complexes such as [Ru-(bdmpza)$(Cl)_2(NO)]$ (1868 cm^{-1} (CH_2Cl_2) and 1872 cm^{-1} (KBr)) and $[Ru(bdmpza)_2(NO)]Cl$ (1862 cm^{-1} (CH_2Cl_2) and 1860 cm^{-1} (KBr)), which have been reported recently by Cao and Otero, have been observed at much lower wavenumbers compared to the $\tilde{\nu}$(NO) of **13a,b** and **14a-c** (Table 11).[5]

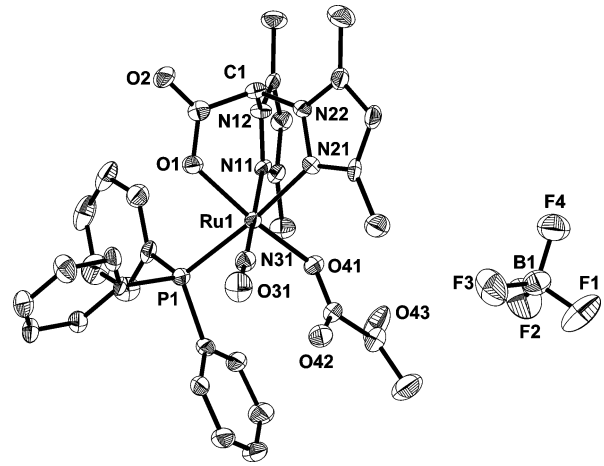

Figure 14. Molecular structure of $[Ru(bdmpza)(O_2CC(O)Me)(NO)(PPh_3)]BF_4$ (**14a**) with thermal ellipsoids drawn at the 50% probability level. Hydrogen atoms and solvent molecules are omitted for clarity.

Crystals suitable for X-ray structure determination have been obtained for complex **14a**. The molecular structure of $[Ru(bdmpza)(O_2CC(O)Me)(NO)(PPh_3)]BF_4$ (**14a**) (Figure 14, Table 10) exhibits a complex geometry with the NO *trans* to a pyrazolyl donor and a κO^1-coordination of the 2-oxocarboxylato ligand *trans* to the carboxylate donor of the bdmpza ligand. The distances and angles of the [Ru(bdmpza)(PPh_3)] fragment agree well with those of the structures **2a** × H_2O and **3c**.

The torsion angle ∠(O(41)−C(41)−C(42)−O(43)) of the 2-oxocarboxylato ligand in **14a** (−18.5(7)°) is bigger than in the benzoylformato complex **3c** [−0.3(5)°], but a conjugation across the π system of the 2-oxocarboxylato ligand should still be possible. The bond distances of the nitrosyl ligand are d(Ru−NO) = 1.760(4) Å and d(N−O) = 1.145(4) Å in **14a**, and the nitrosyl ligand is close to linear with ∠(Ru−N−O) = 177.4(4)°. These values agree well with those of the ruthenium(II) Cp and Tp nitrosyl complexes (Table 11).

Summary and Prospects

Many preparative and structural studies have demonstrated the versatility of the complexes [Ru(bdmpza)-$(O_2CR)(PPh_3)]$ (**2a**, **2b**) and [Ru(bdmpza)$(O_2C(CO)R)$-$(NO)(PPh_3)]$ (**3a**-**c**) as 16 VE fragments with hemilabile κ^2-coordinating carboxylato and 2-oxocarboxylato ligands.

(41) Enemark, J. H.; Feltham, R. D. *Coord. Chem. Rev.* **1974**, *13*, 339–406; Mononitrosyl complexes are described by $\{RuNO\}^n$, where n is the number of d electron on ruthenium when the NO is formally bound as NO^+

(42) McCleverty, J. A. *Chem. Rev.* **2004**, *104*, 403–418.

Solvent molecules (pyridine, acetonitrile) as well as small molecules and ions (CO, SO_2, NO^+) have been coordinated to a [Ru(bdmpza)(O_2CR)(PPh_3)] fragment. The chances of generating otherwise unstable compounds in the protecting environment of the new transition metal fragments seem quite promising. Future studies will be able to build on these results and might expand them to an activation of small molecules. Correlations between structure and reactivity are beginning to be recognized with a higher reactivity of the κ^2-carboxylato complexes compared to that of the 2-oxocarboxylato complexes.

Acknowledgment. We gratefully acknowledge financial support by the Deutsche Forschungsgemeinschaft through SFB 583 "Redox-active metal complexes" and the Fonds der Chemie. The authors thank Prof. Dr. H. Fischer for support and discussion and the Degussa AG for a generous gift of rutheniumtrichloride hydrate.

Supporting Information Available: Crystallographic information files (CIF). This material is available free of charge via the Internet at http://pubs.acs.org.

IC8000224